Collège de France, 18 Dec 2013

Observation of second sound and more recent developments in ultracold Fermi gases

Rudolf Grimm

"Center for Quantum Physics" in Innsbruck

Inst. Expt. Physics, U Innsbruck

IQOQI - Austrian Academy of Sciences

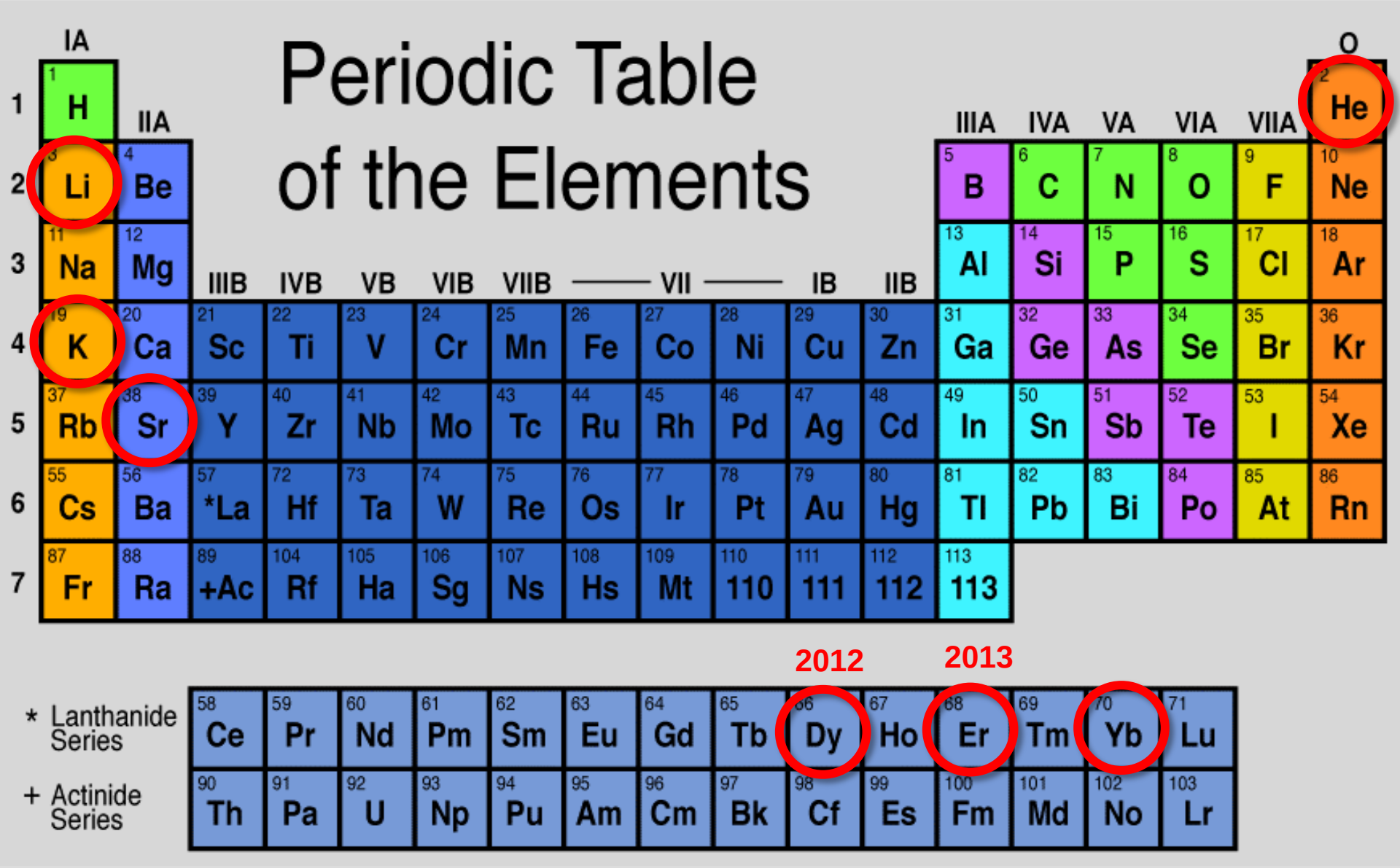
Periodic Table of the Elements
IA
IIA
IIIB
IVB
VB
VIB
VIIB
VII
IB
IIB
IIIA
IVA
VA
VIA
VIIA
O
1 H
2 He
3 Li
4 Be
5 B
6 C
7 N
8 O
9 F
10 Ne
11 Na
12 Mg
13 Al
14 Si
15 P
16 S
17 Cl
18 Ar
19 K
20 Ca
21 Sc
22 Ti
23 V
24 Cr
25 Mn
26 Fe
27 Co
28 Ni
29 Cu
30 Zn
31 Ga
32 Ge
33 As
34 Se
35 Br
36 Kr
37 Rb
38 Sr
39 Y
40 Zr
41 Nb
42 Mo
43 Tc
44 Ru
45 Rh
46 Pd
47 Ag
48 Cd
49 In
50 Sn
51 Sb
52 Te
53 I
54 Xe
55 Cs
56 Ba
57 *La
72 Hf
73 Ta
74 W
75 Re
76 Os
77 Ir
78 Pt
79 Au
80 Hg
81 Tl
82 Pb
83 Bi
84 Po
85 At
86 Rn
87 Fr
88 Ra
89 +Ac
104 Rf
105 Ha
106 Sg
107 Ns
108 Hs
109 Mt
110 110
111 111
112 112
113 113
2012
2013
* Lanthanide Series
+ Actinide Series
58 Ce
59 Pr
60 Nd
61 Pm
62 Sm
63 Eu
64 Gd
65 Tb
66 Dy
67 Ho
68 Er
69 Tm
70 Yb
71 Lu
90 Th
91 Pa
92 U
93 Np
94 Pu
95 Am
96 Cm
97 Bk
98 Cf
99 Es
100 Fm
101 Md
102 No
103 Lr

degenerate Fermi gases

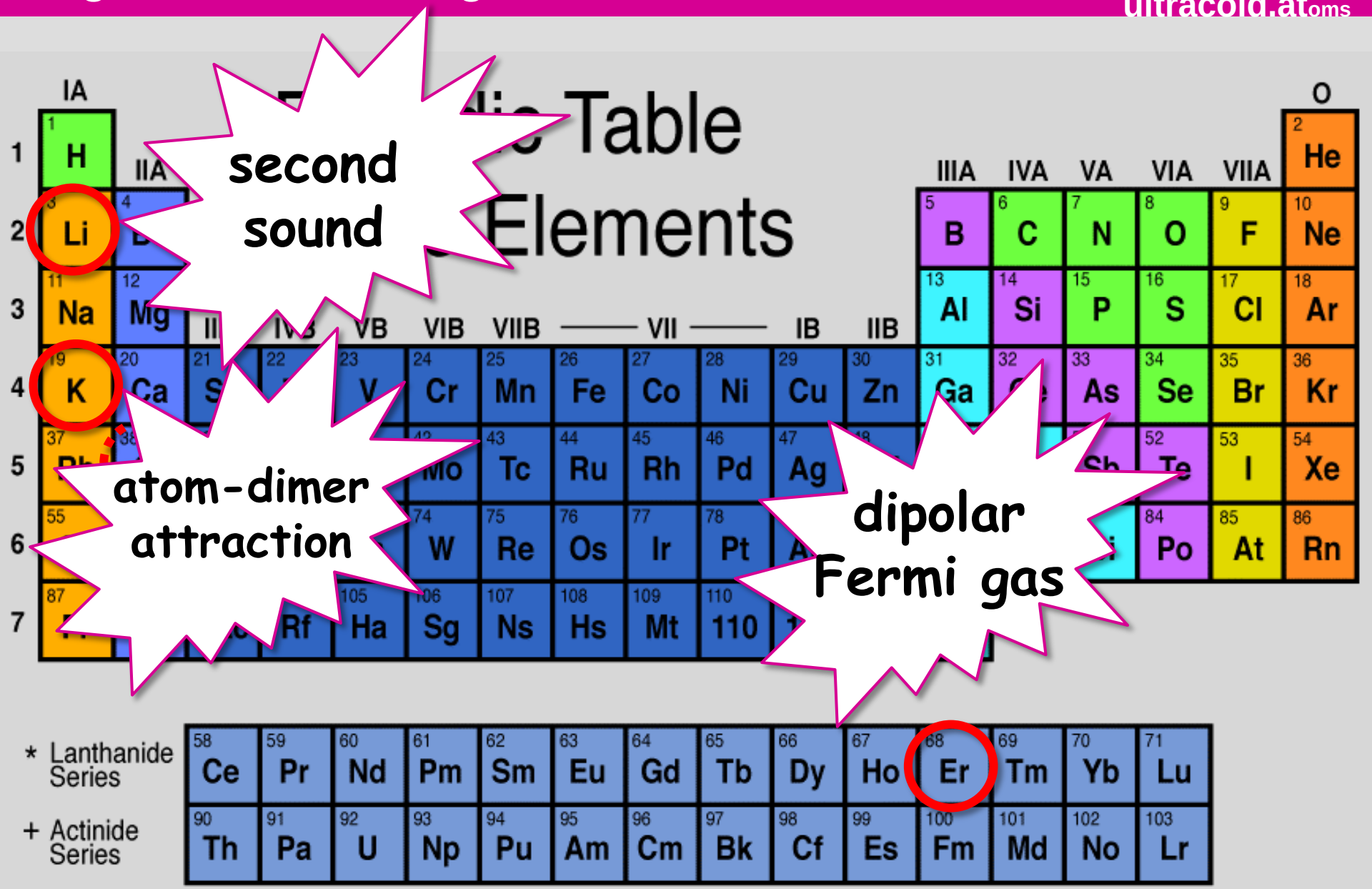

Liquid helium II

1963 film by Alfred Leitner

https://www.youtube.com/watch?v=OIcFSHAz4E8

#2: enormous heat conductivity

#3: zero viscosity, or not zero?

#4: fountain effect

#5: Rollin film

#6: **second sound**

bizarre phenomena explained in terms of **two-fluid hydrodynamics**

Tisza (1938), Landau (1941)

(another famous effect: quantized vortices)

two-fluid model

normal part (carries all entropy)

n n n n n n n n n n n n n n n n n n n n

s s s s s s s s s s s s s s s s s s s s

superfluid part (no entropy)

temperature $\rightarrow$ superfluid fraction **s**/(**n**+**s**)

theoretical framework:
two-fluid hydrodynamics
Landau (1941)

n n n n n n n n n n n n n n n n n n n n

s s s s s s s s s s s s s s s s s s s s

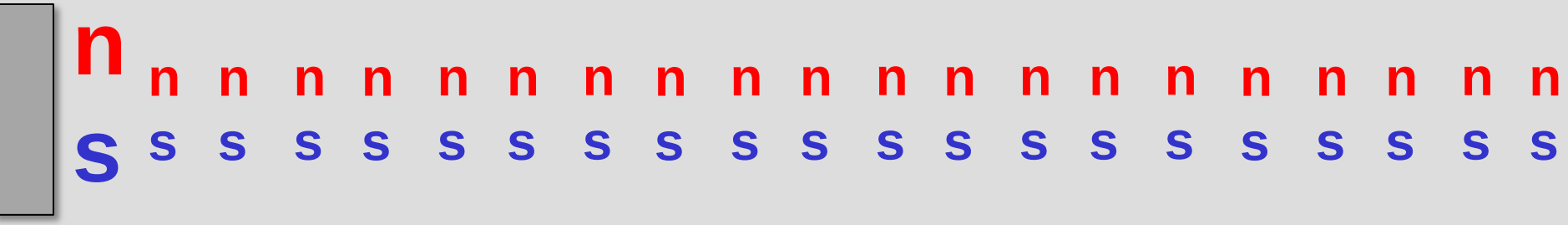
n n n n n n n n n n n n n n n n n n n
s s s s s s s s s s s s s s s s s s s

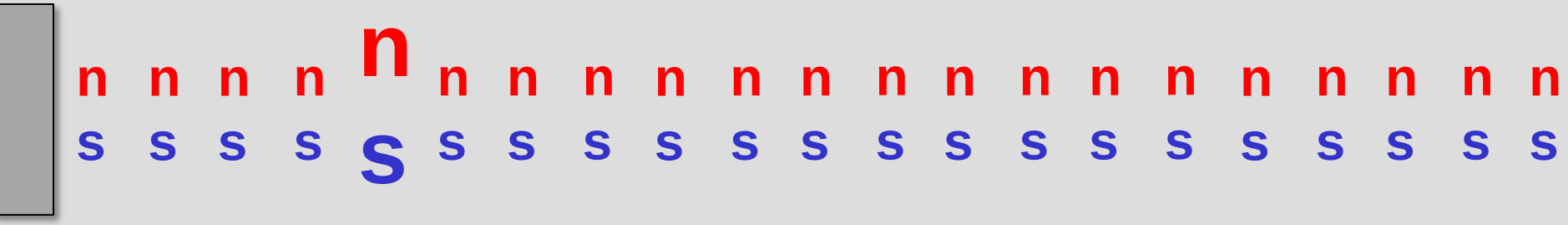
n n n n n n n n n n n n n n n n n n n n
s s s s s s s s s s s s s s s s s s s s

sound

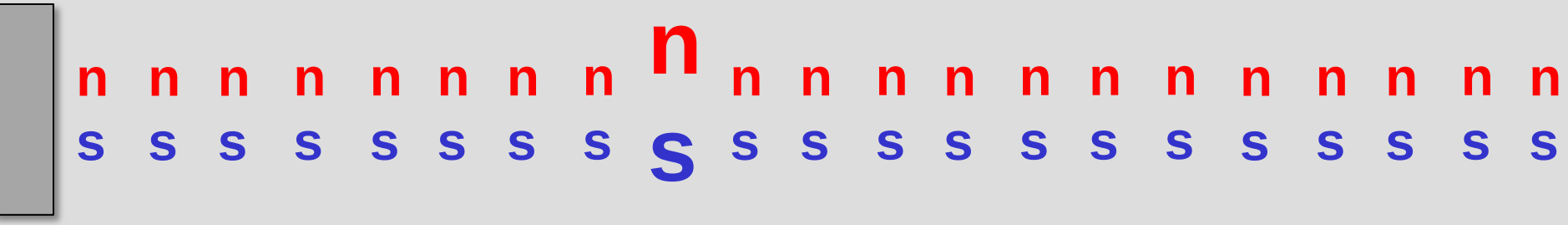

ordinary sound:
pressure wave
(adiabatic)

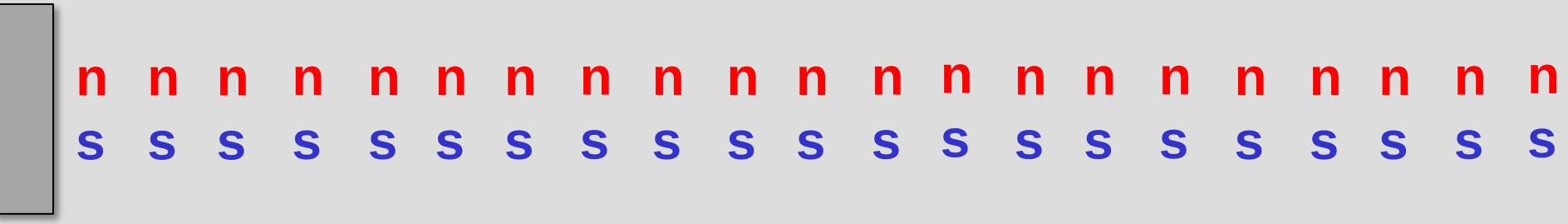
n n n n n n n n n n n n n n n n n n n n
s s s s s s s s s s s s s s s s s s s s

n n n n n n n n n n n n n n n n n n n

s s s s s s s s s s s s s s s s s s s

sound

n n n n n n n n n n n n n n n n n n n n n

s s s s s s s s s s s s s s s s s s s s s

sound

n n n n n n n n n n n n n n n n n n n n n

s s s s s s s s s s s s s s s s s s s s s

n n n n n n n n n n n n n n n n n n n n n

s s s s s s s s s s s s s s s s s s s s s

sound

n n n n n n n n n n **n** n n n n n n n n n n n

s s s s s s s s s s s s s s s s s s s s s s s

second sound:
entropy wave
(at constant pressure)

second sound in He II: detection

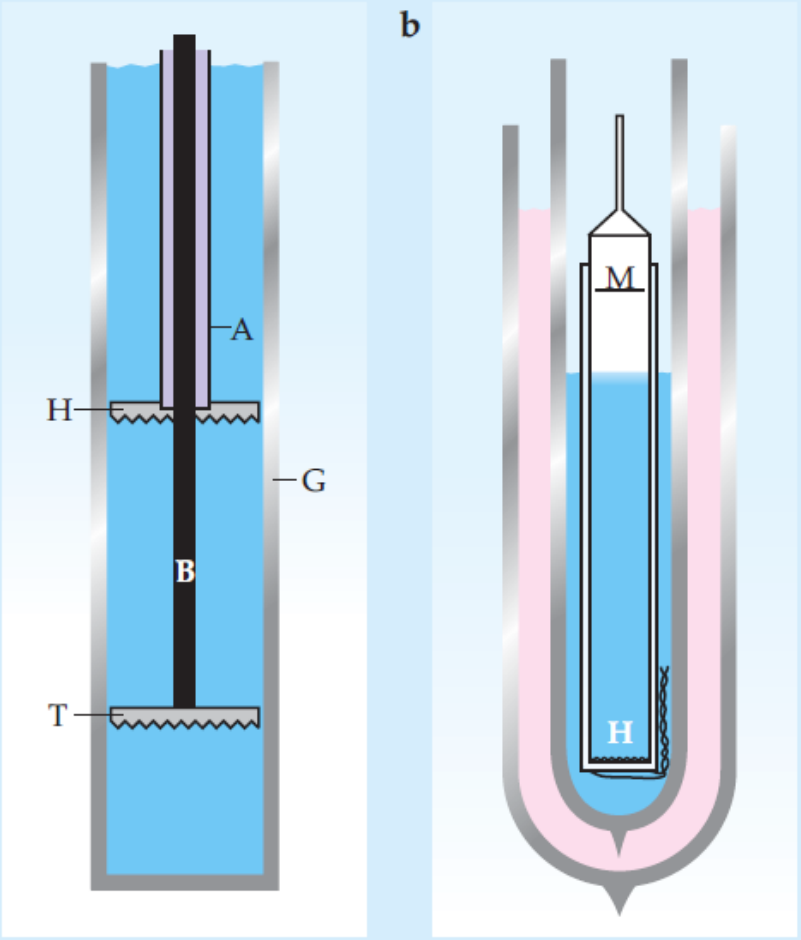

Figure 3. Detecting second sound. (a) Resonator used by Vasilii Peshkov in 1948 to study standing waves of second sound in helium II. The glass tube G is closed at the bottom and acts as a resonator. The heater H is mounted on a glass disk that can be moved up and down by the tube A. The thermometer T is an open winding of phosphor bronze wire on a frame movable by tube B. An electrical current of frequency *f* generates small temperature fluctuations of frequency 2*f*. The thermometer T can be moved up and down to trace out the standing wave patterns of second sound, from which the velocity of second sound can be measured. In 1960 Peshkov used a similar apparatus attached to a helium-3 refrigerator to reach temperatures as low as 0.4 K. (Adapted from ref. 6.) **(b)** Apparatus used at Yale University to detect second sound by Lars Onsager's method. A thin lucite tube was inserted into liquid helium (blue) in a dewar surrounded by liquid nitrogen (pink). A heater H at the bottom of the tube was excited at 1 kHz, and a microphone M in the vapor above the liquid was tuned to 2 kHz and its signal rectified. As the liquid helium bath evaporated, the free surface fell and resonant peaks appeared from the microphone output, from which the velocity of second sound could be deduced. (Adapted from ref. 7.)

illustration from R. J. Donnelly, Phys. Today, Oct. 2009

resonantly interacting spin mixture of ^{6}Li

since the early experiments in 2003/04
a well-established system to study
BEC-BCS crossover, fermion superfluidity, and
many many many related topics

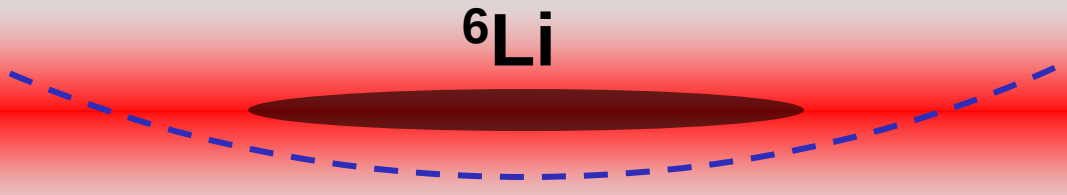

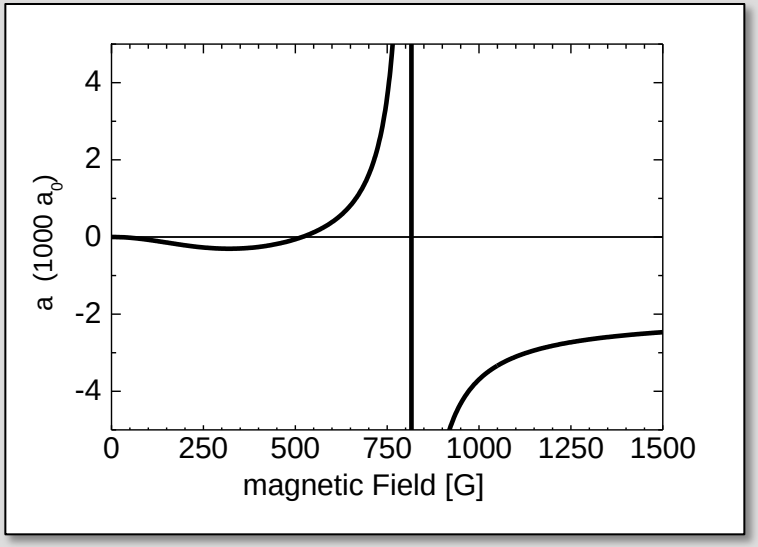

hybrid trap:
optical conf. radially
magnetic conf. axially

expt. (1997): sound propagation in BEC

VOLUME 79, NUMBER 4 PHYSICAL REVIEW LETTERS 28 JULY 1997

Propagation of Sound in a Bose-Einstein Condensate

M. R. Andrews, D. M. Kurn, H.-J. Miesner, D. S. Durfee, C. G. Townsend, S. Inouye, and W. Ketterle

Department of Physics and Research Laboratory of Electronics, Massachusetts Institute of Technology, Cambridge, Massachusetts 02139

(Received 20 March 1997; revised manuscript received 27 May 1997)

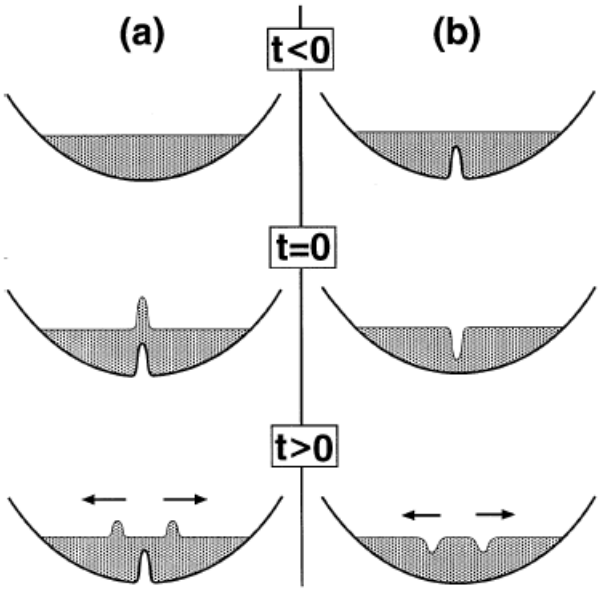

FIG. 1. Excitations of wave packets in a Bose-Einstein condensate. A condensate is confined in the potential of a magnetic trap. At time $t = 0$, a focused, blue-detuned laser beam is suddenly switched on (a) or off (b) and, by the optical dipole force, creates, respectively, two positive or negative pertubations in density which propagate at the speed of sound.

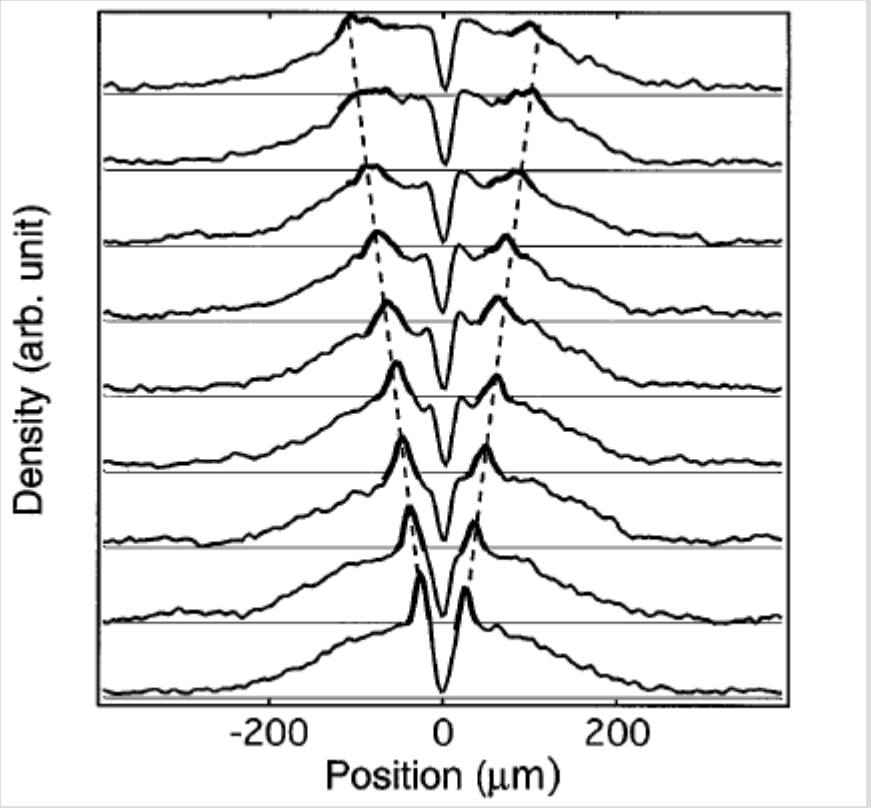

expt. (2007): sound prop. in resonant FG

PRL 98, 170401 (2007) PHYSICAL REVIEW LETTERS week ending 27 APRIL 2007

Measurement of Sound Velocity in a Fermi Gas near a Feshbach Resonance

J. Joseph, B. Clancy, L. Luo, J. Kinast, A. Turlapov, and J. E. Thomas*
Department of Physics, Duke University, Durham, North Carolina, 27708, USA
(Received 21 December 2006; published 24 April 2007)

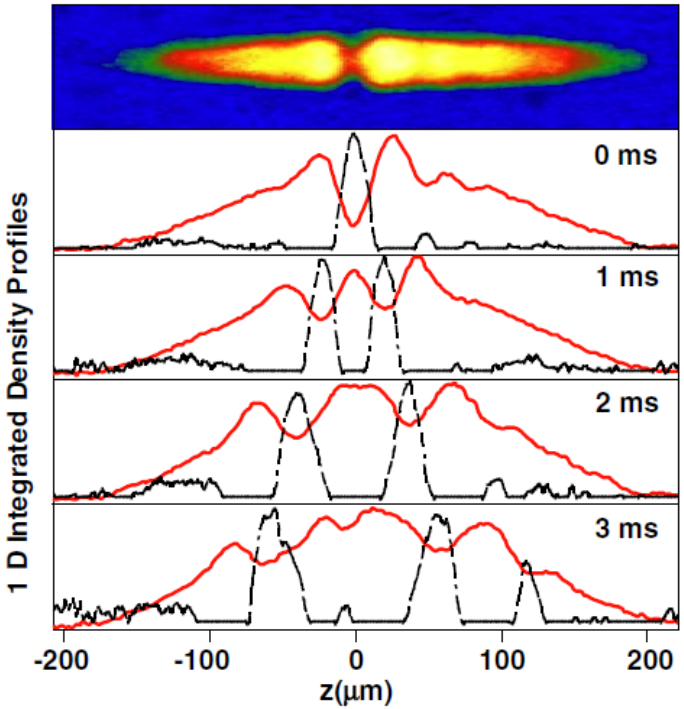

FIG. 1 (color online). Sound propagation at the Feshbach resonance: (Top) 2D density profile showing initial perturbation. (Bottom) Gray (red) solid curve: Axial density profiles of the cloud for different in-trap propagation times; black dashed curve: valleys (inverted).

ordinary (‘first’) sound

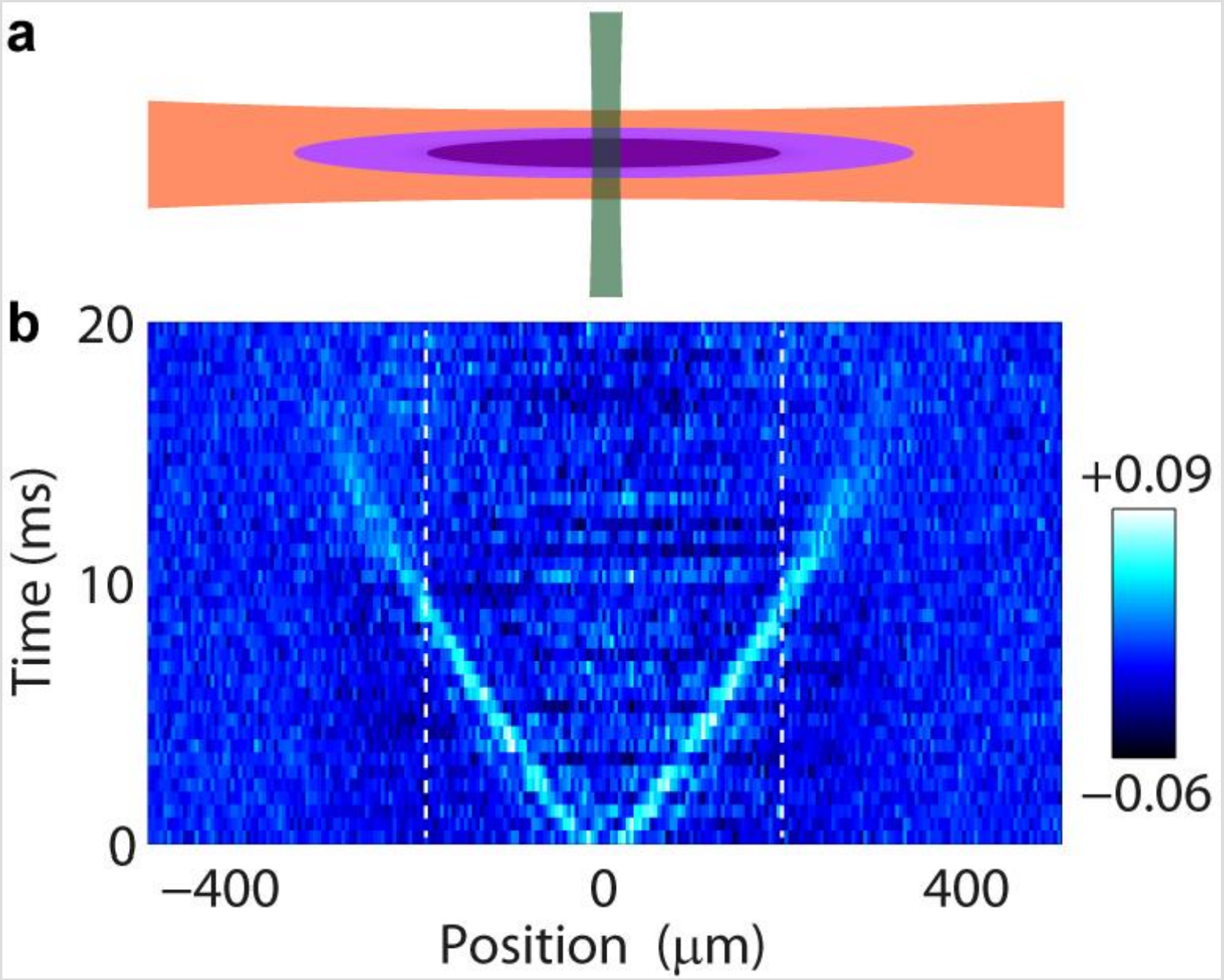

change excitation scheme

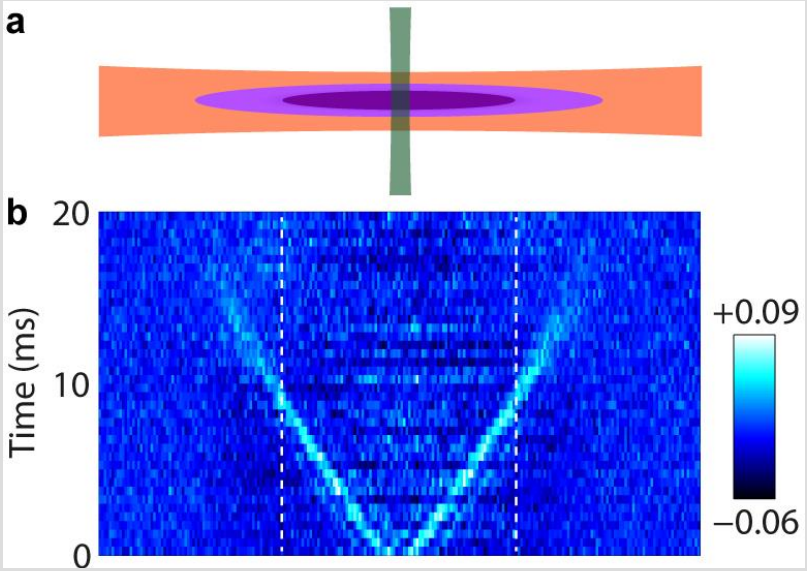

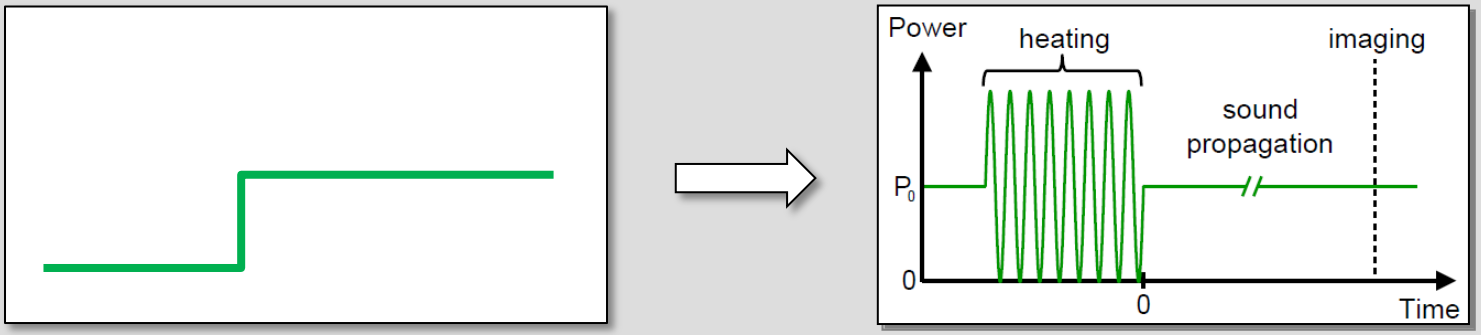

propagation of first and second sound

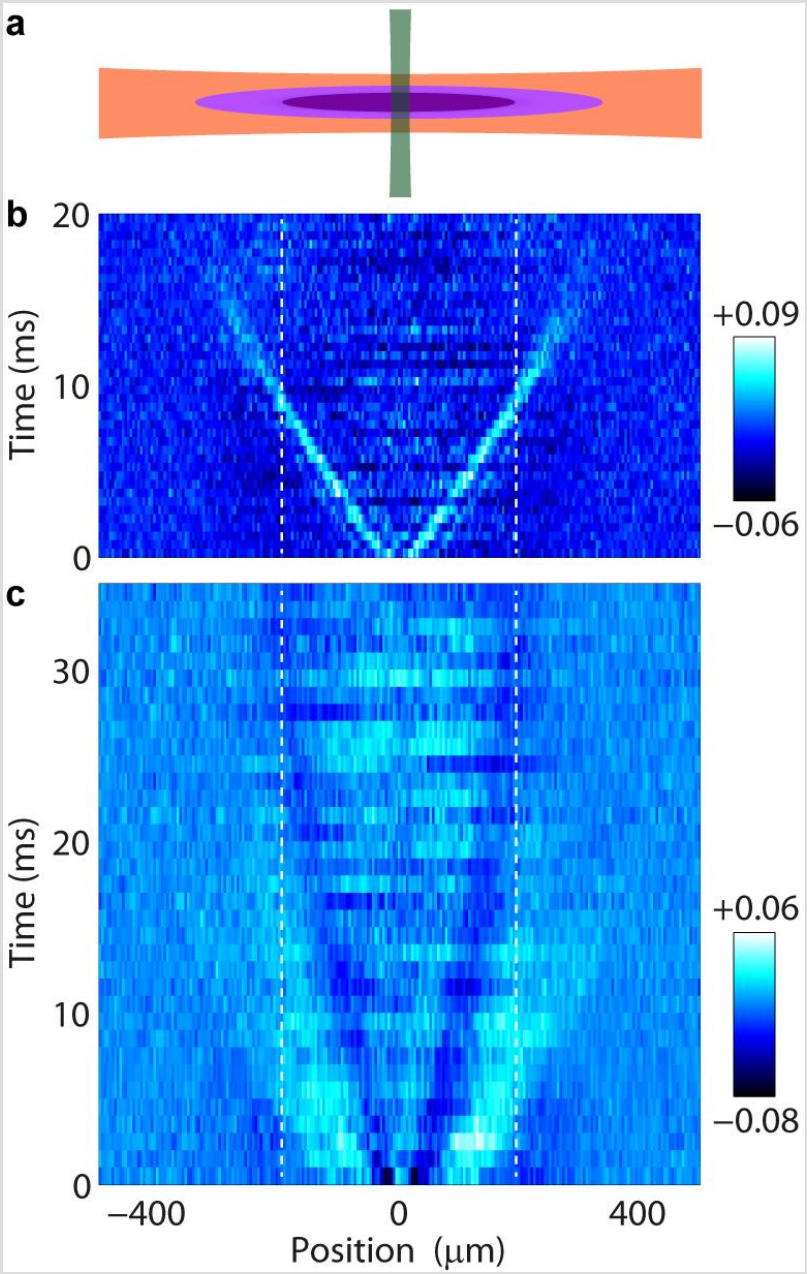

local heat pulse appears as a **dip**

pulse position vs. time

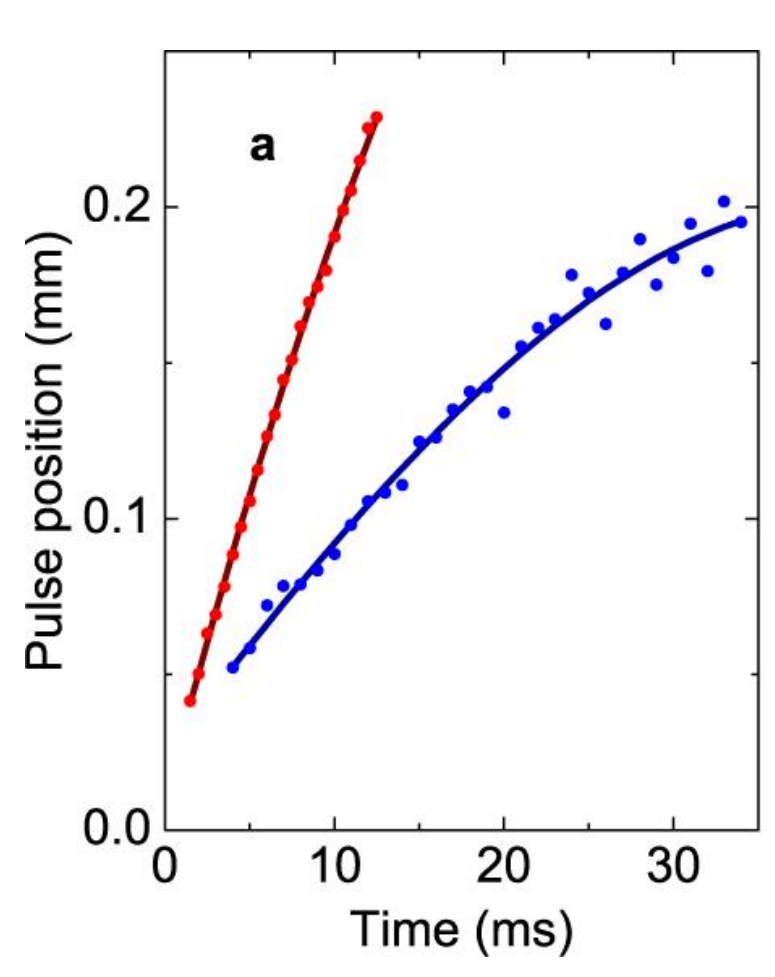

extracting the sound speeds

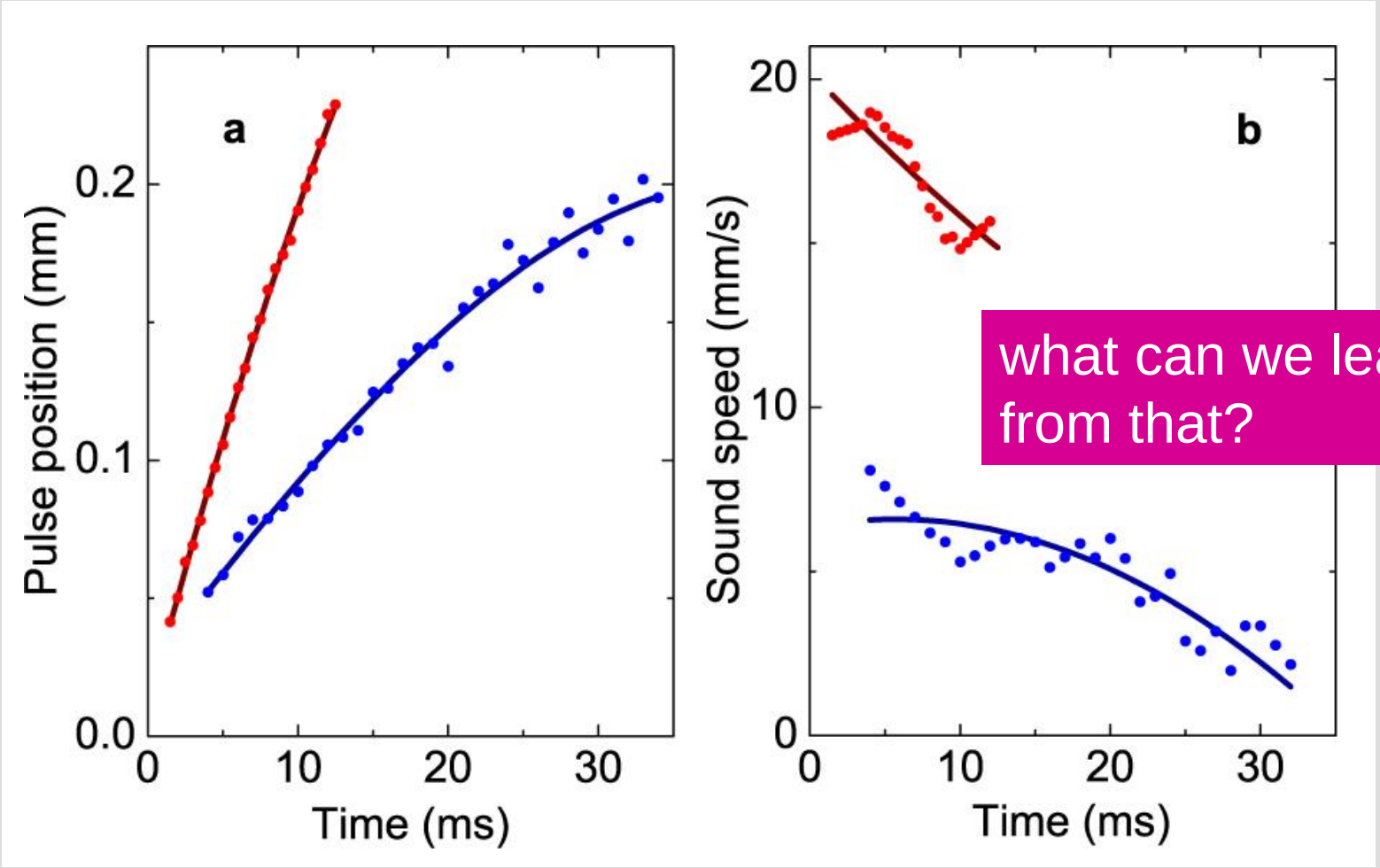

what can we learn from that?

Innsbruck-Trento team: expt. and theory!

ultracold.atoms

Innsbruck-Trento team: expt. and theory!

22.01.2013

LETTER Nature **498**, 78 (2013)

doi:10.1038/nature12136

Second sound and the superfluid fraction in a Fermi gas with resonant interactions

Leonid A. Sidorenkov[1,2], Meng Khoon Tey[1,2], Rudolf Grimm[1,2], Yan-Hua Hou[3], Lev Pitaevskii[3,4] & Sandro Stringari[3]

personal connection to Landau

two important theory papers from Trento

PRL 105, 150402 (2010) PHYSICAL REVIEW LETTERS week ending 8 OCTOBER 2010

First and Second Sound in Cylindrically Trapped Gases

G. Bertaina,[1] L. Pitaevskii,[1,2] and S. Stringari[1]
[1]*INO-CNR BEC Center and Dipartimento di Fisica, Università di Trento, I-38123 Povo, Trento, Italy*
[2]*Kapitza Institute for Physical Problems, Kosygina 2, 119334 Moscow, Russia*
(Received 29 January 2010; revised manuscript received 1 September 2010; published 4 October 2010)

effective 1D thermodynamic framework to solve Landau's hydrodynamic equations for our trap geometry

PHYSICAL REVIEW A 88, 043630 (2013)

First and second sound in a highly elongated Fermi gas at unitarity

Yan-Hua Hou,[1] Lev P. Pitaevskii,[1,2] and Sandro Stringari[1]
[1]*Dipartimento di Fisica, Università di Trento and INO-CNR BEC Center, I-38123 Povo, Italy*
[2]*Kapitza Institute for Physical Problems RAS, Kosygina 2, 119334 Moscow, Russia*
(Received 28 June 2013; published 21 October 2013)

describes behavior of 1D thermodyn. quantities based on EOS from MIT (Zwierlein group)

thermal expansion

Hou et al., PRA **88**, 043630 (2013)

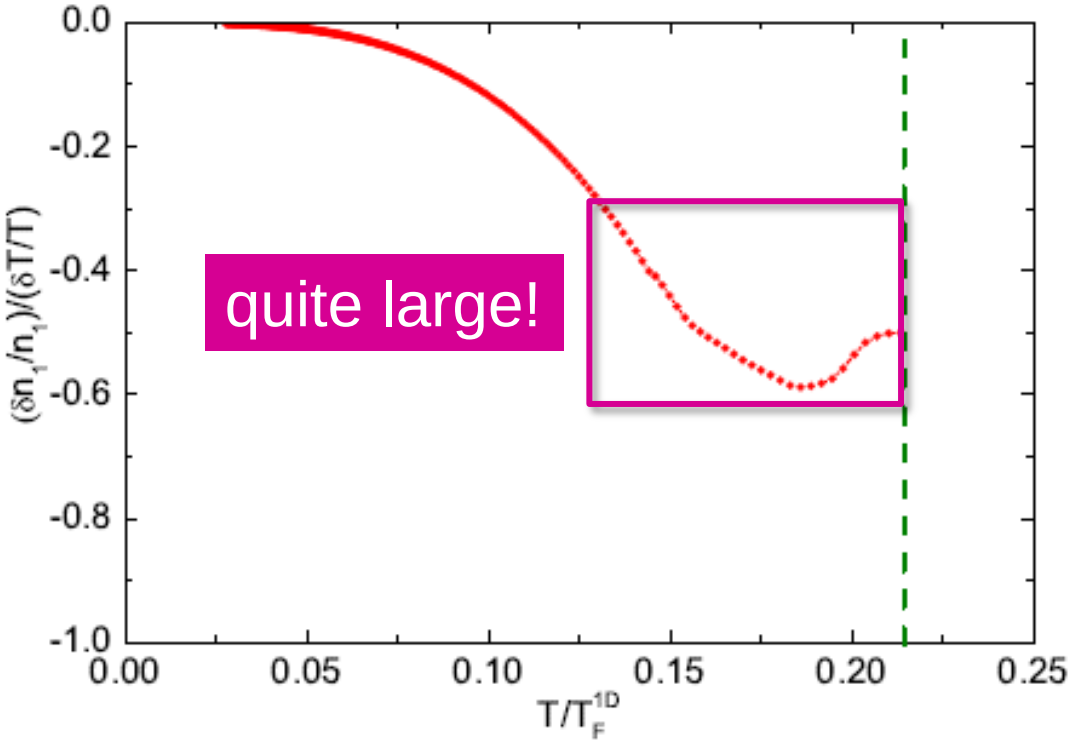

this is why a local heat pulse appears as a density dip !

relevant Fermi temperature

2D harmonic trap (uniform along z-axis)

on-axis Fermi energy: natural energy scale

$$E_F = \left[\frac{15\pi}{4}\left(\frac{\hbar^2}{2m}\right)^{3/2} m\omega^2\, n_1\right]^{2/5}$$

Bertaina et al.,
PRL 105, 150402 (2010)

relevant Fermi temperature

3D harmonic trap (weak confinement along z-axis)

on-axis Fermi energy: natural energy scale

$$E_F = \left[\frac{15\pi}{4}\left(\frac{\hbar^2}{2m}\right)^{3/2} m\omega^2\, n_1\right]^{2/5}$$

Bertaina et al.,
PRL 105, 150402 (2010)

relevant Fermi temperature

3D harmonic trap (weak confinement along z-axis)

on-axis Fermi energy: natural energy scale

$$E_F = \left[\frac{15\pi}{4}\left(\frac{\hbar^2}{2m}\right)^{3/2} m\omega^2\, n_1\right]^{2/5}$$

z-dependent

define corresponding Fermi temp. $T_F^{1D}(z)$

T/T_F^{1D} varies along trap axis

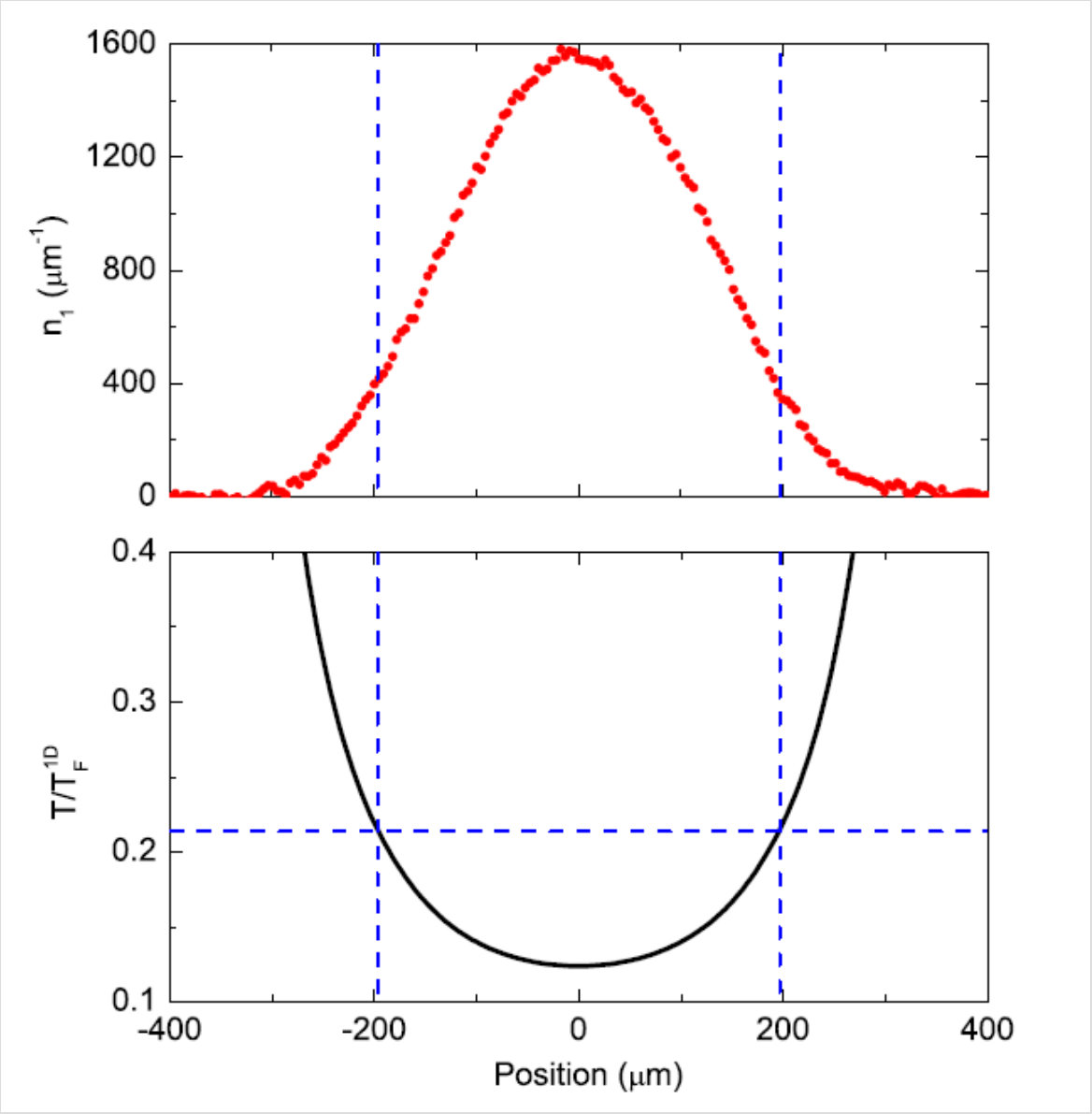

sound speeds in terms of reduced quantities

first-sound speed:

excellent agreement with calculation based on known EOS

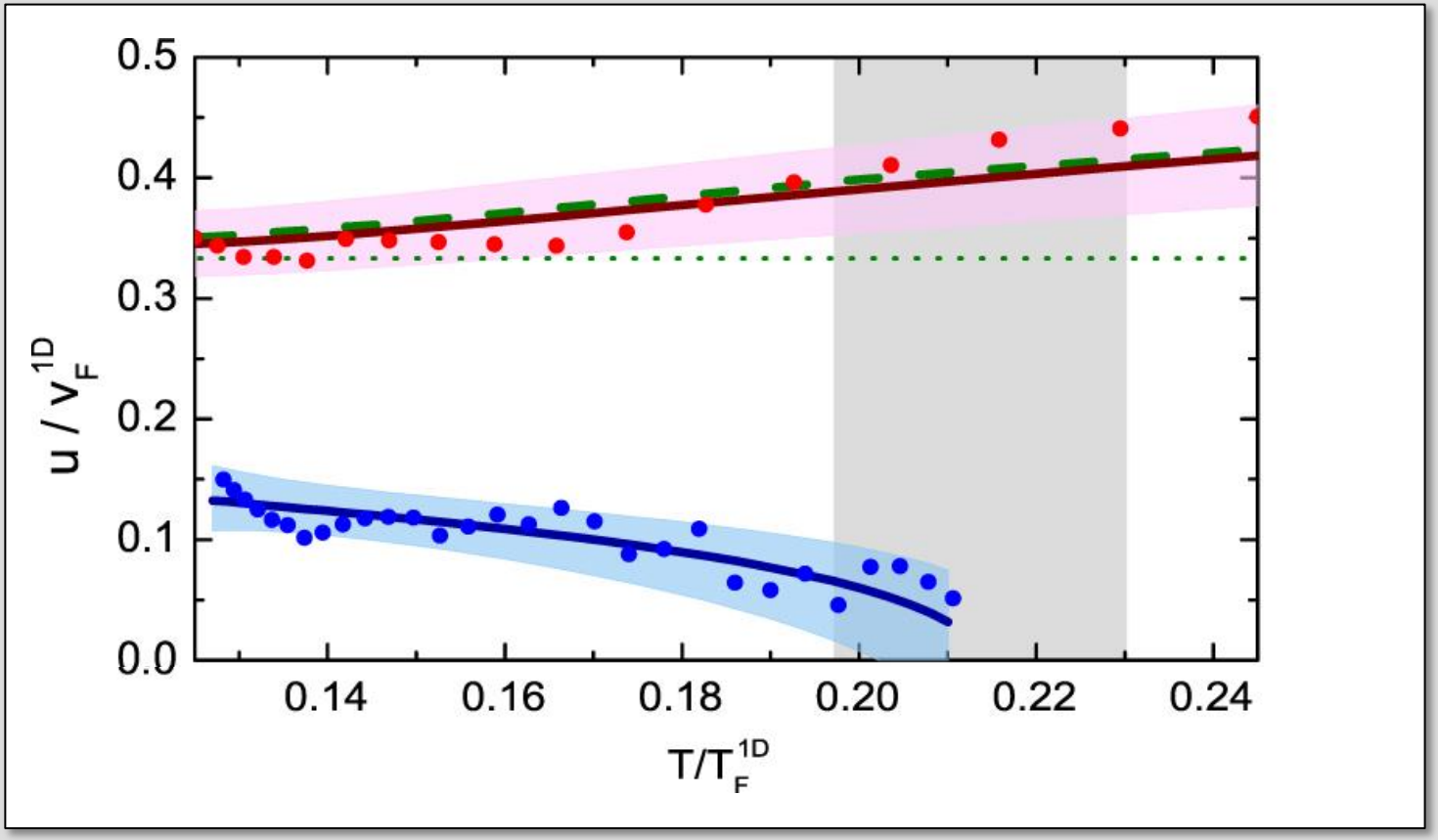

speed of the other signal:

strong temperature dependence, goes to zero near T_c

Landau's result

ТЕОРИЯ СВЕРХТЕКУЧЕСТИ ГЕЛИЯ II

ЖЭТФ, 11, 592, 1941
J. Phys. USSR, 5, 71, 1941

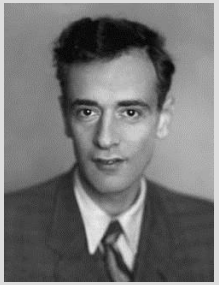

Обозначив общее значение C_p и C_v буквой C, а общее значение $(\partial p/\partial \rho)_T$ и $(\partial p/\partial \rho)_S$ просто как $\partial p/\partial \rho$, получаем из уравнения (8.9) две скорости звука u_1 и u_2 в виде

$$u_1^2 = \frac{\partial p}{\partial \rho}, \qquad u_2^2 = \frac{TS^2\rho_s}{C\rho_n}. \tag{8.10}$$

Таким образом, одна из скоростей (u_1) почти постоянна, а другая (u_2) сильно зависит от температуры, обращаясь в нуль в λ-точке.

yes, this is exactly what we see !!!

sound speeds

according to effective 1D version of Landau's two-fluid theory

$$\frac{u_1}{v_F^{1\mathrm{D}}} = \sqrt{\frac{7}{10}\frac{P_1}{n_1 k_B T_F^{1\mathrm{D}}}}$$

$$\frac{u_2}{v_F^{1\mathrm{D}}} = \sqrt{\frac{T}{2k_B T_F^{1D}}\frac{\bar{s}_1^2}{\bar{c}_{p1}}\frac{n_{s1}}{n_{n1}}}$$

by Trento group

the great unknown

where P_1 denotes the 1D pressure (unit of a force), $\bar{s}_1 = s_1/n_1$ is the entropy per particle, and $\bar{c}_{p1} = T(\partial \bar{s}_1/\partial T)_{p1}$ is the isobaric heat capacity per particle.

superfluid fraction (1D)

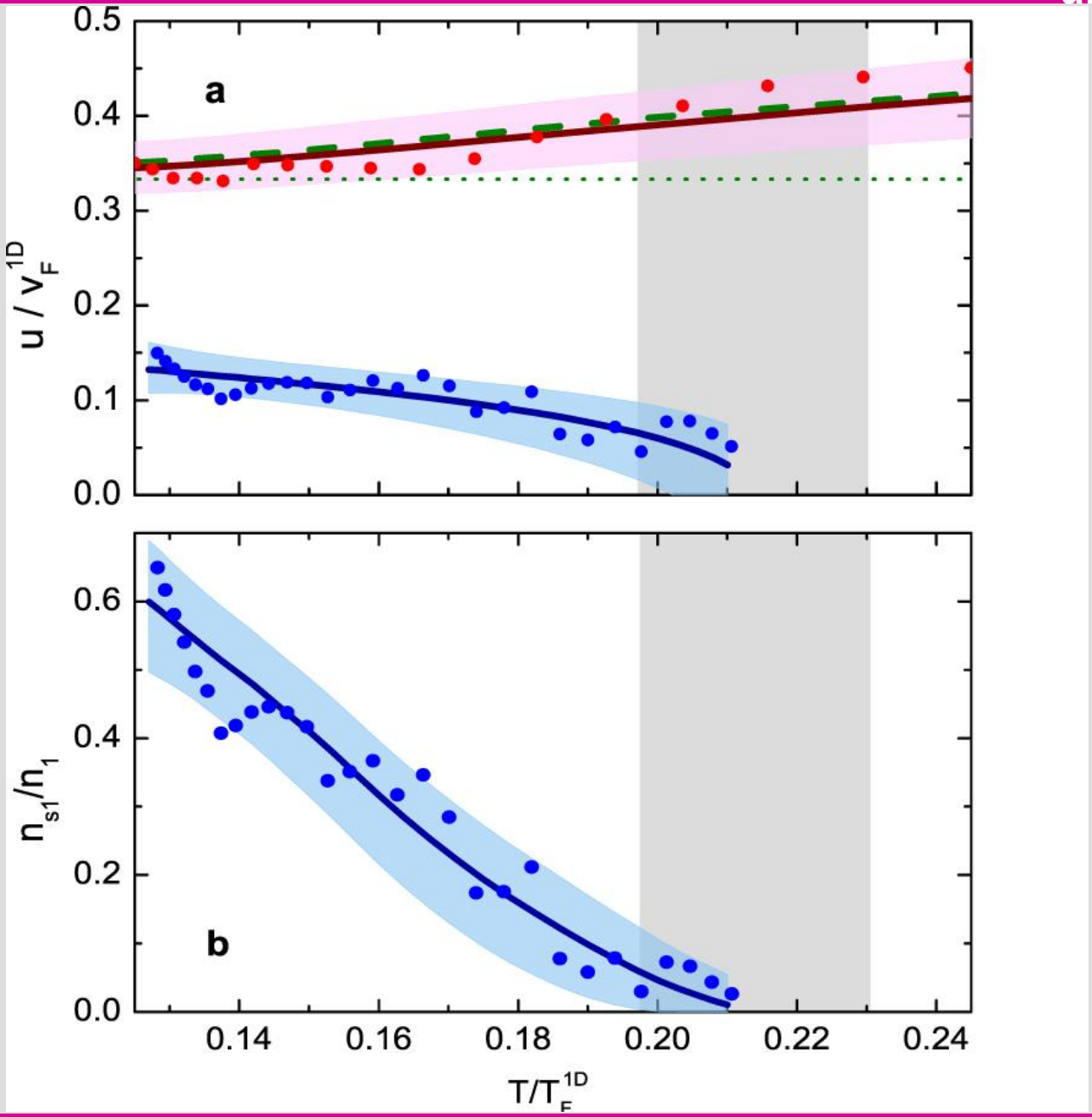

superfluid fraction (uniform gas)

reconstruction based on universal thermodynamics

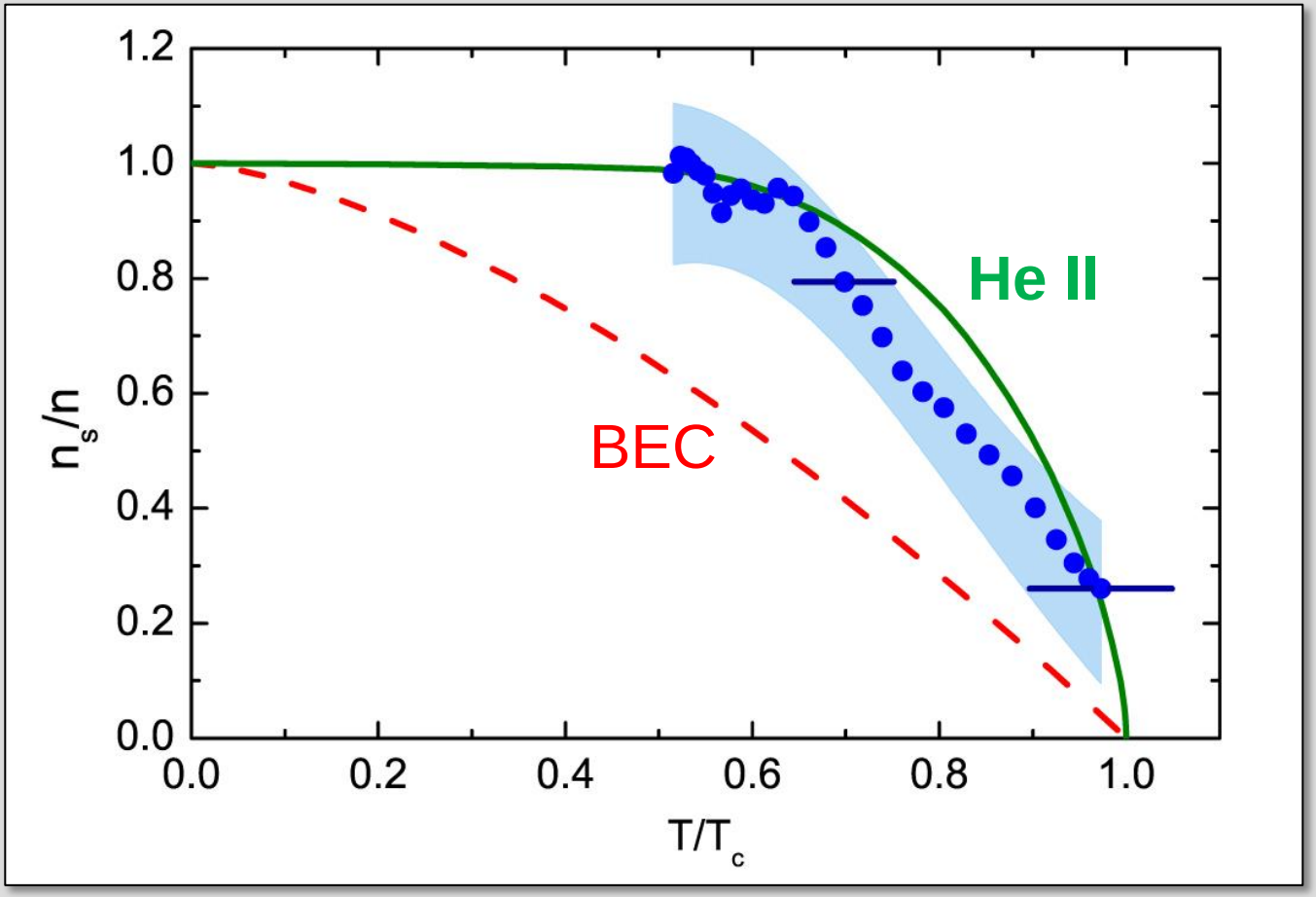

Dash & Taylor, Phys. Rev. 105, 7 (1957)

resonant Fermi gas remarkably close to liquid helium II

comparing with theory?

Taylor et al.,
PRA 77, 033608 (2008)

Salasnich,
PRA 83, 063619 (2010)

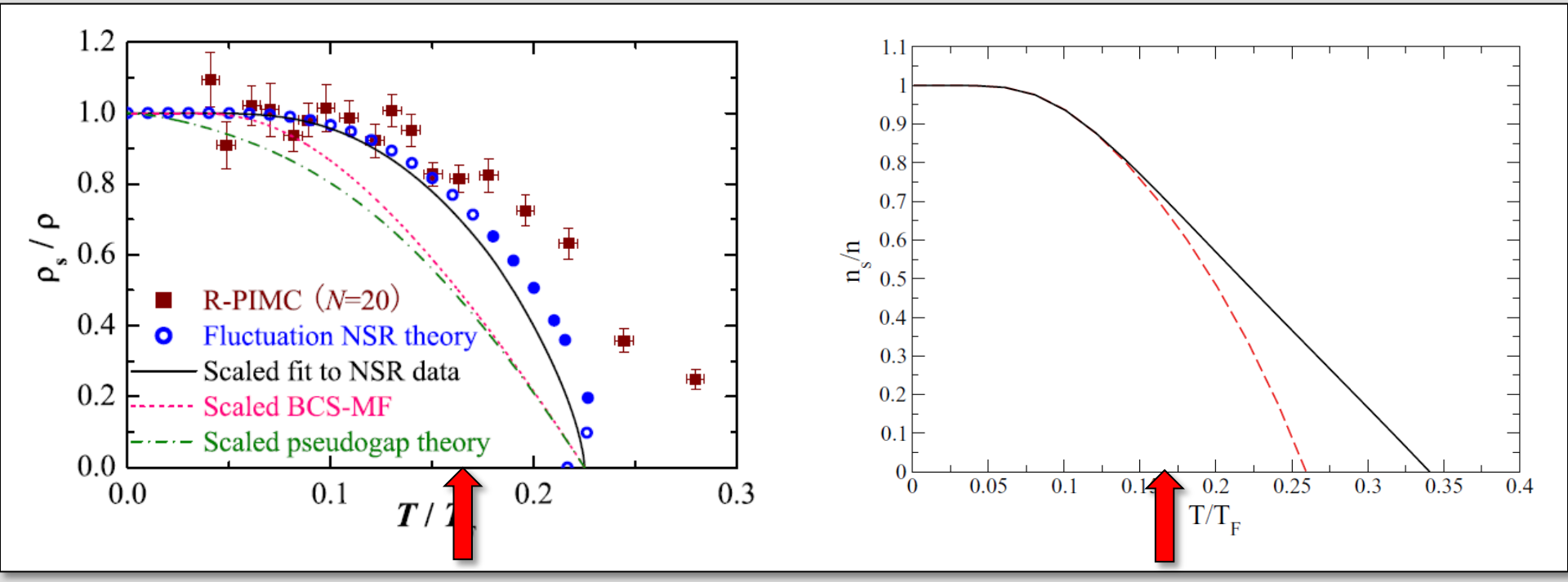

quantum Monte Carlo gives right T_c,
but no information on superfluid fraction!

outlook

be inspired by He II

two-fluid hydrodynamics and transport phenomena revisited

e.g. transport through narrow channels (capillaries)

do things you cannot do with He II

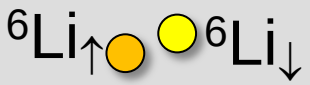

second sound in the BEC-BCS crossover

controlled spin imbalance

low-D and lattices

more exotic superfluids
(e.g., mixed-species systems)

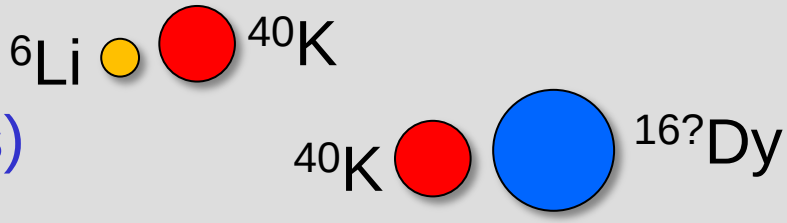

http://www.tirol.tl/images/cms/1303130110D_020_SpeicherZillergruendl_Staumauer.jpg

centrifugal barrier: two regimes

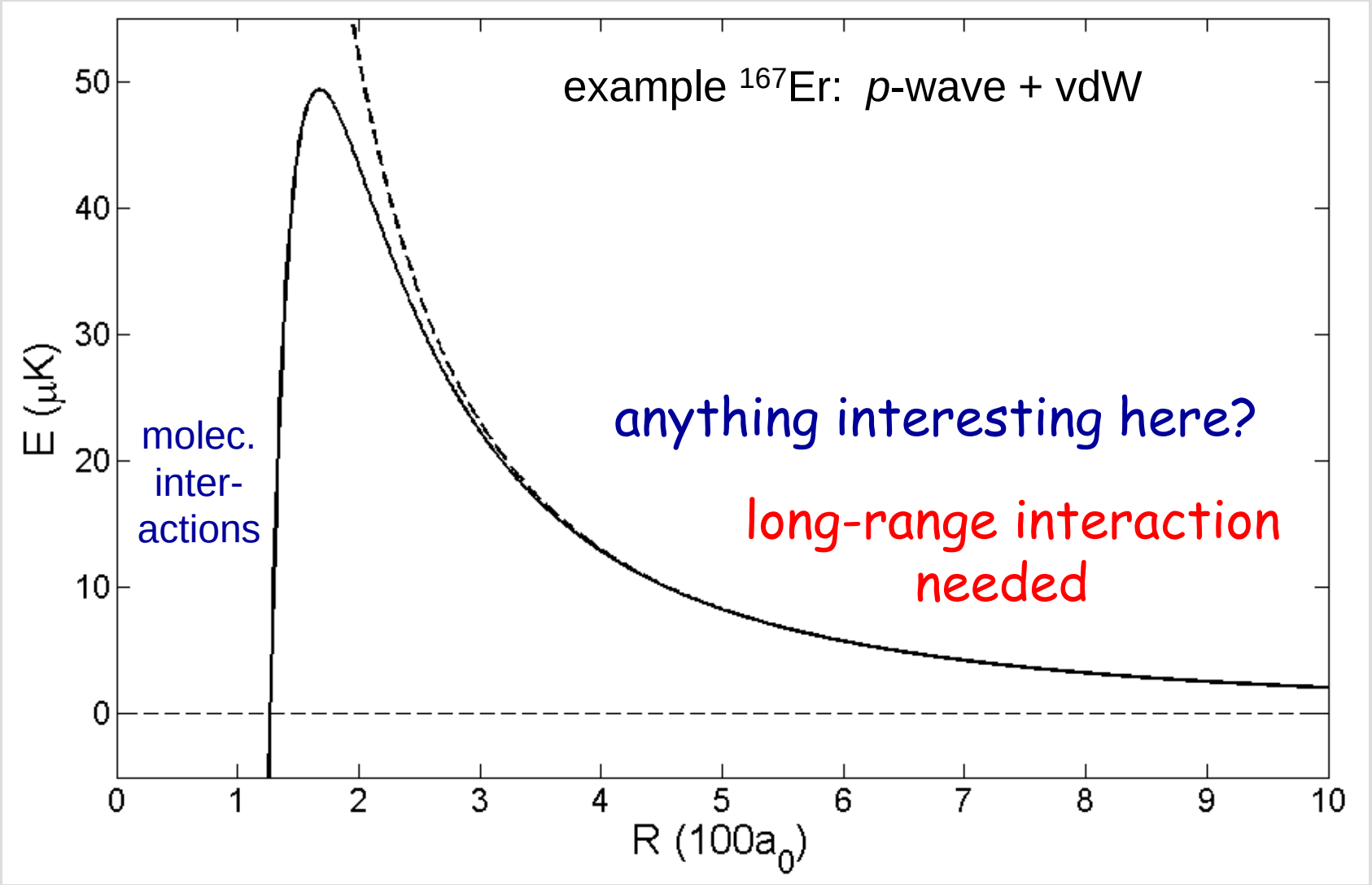

Innsbruck erbium team

ultracold.atoms

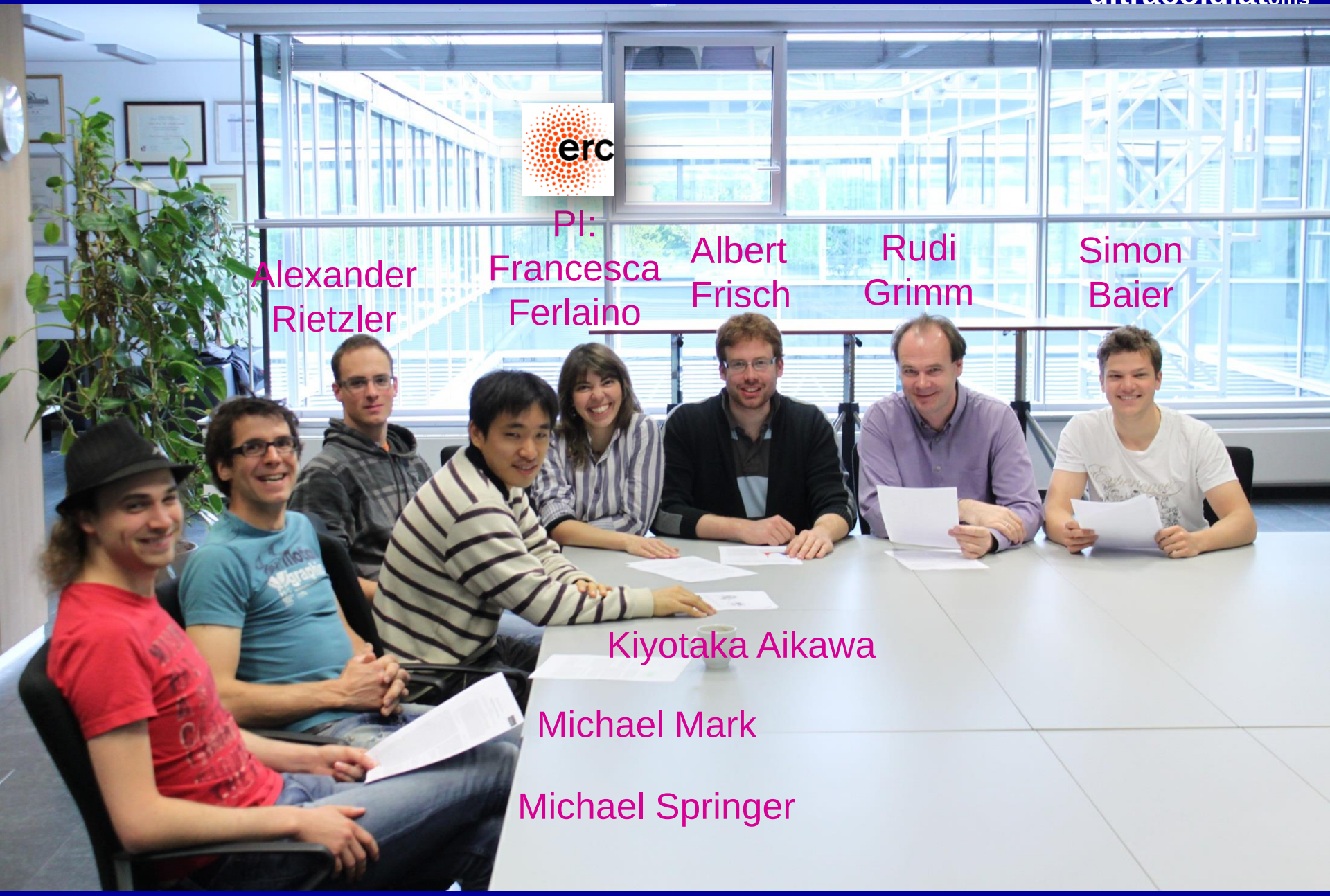

centrifugal barrier: two regimes

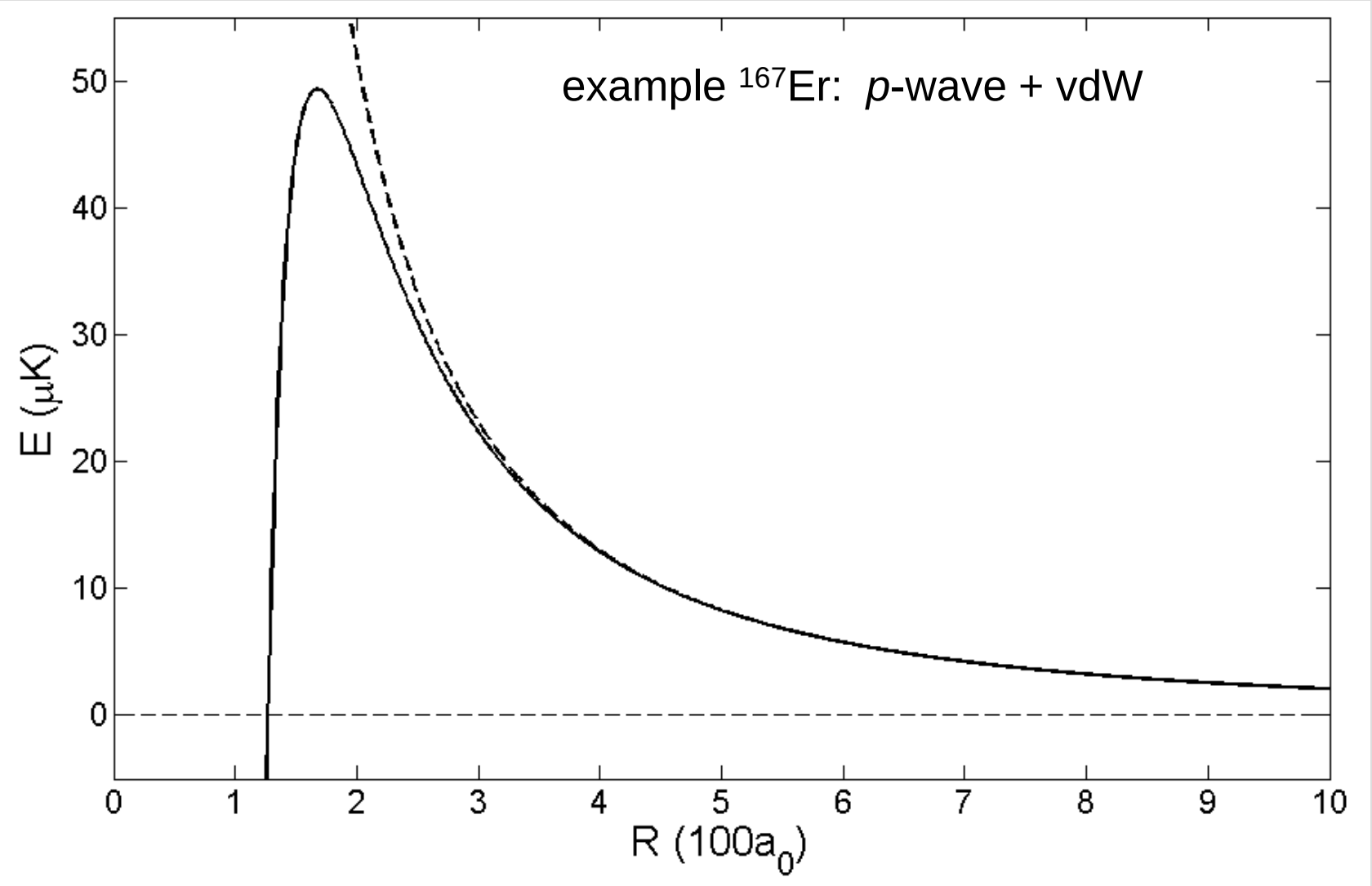

centrifugal barrier: two regimes

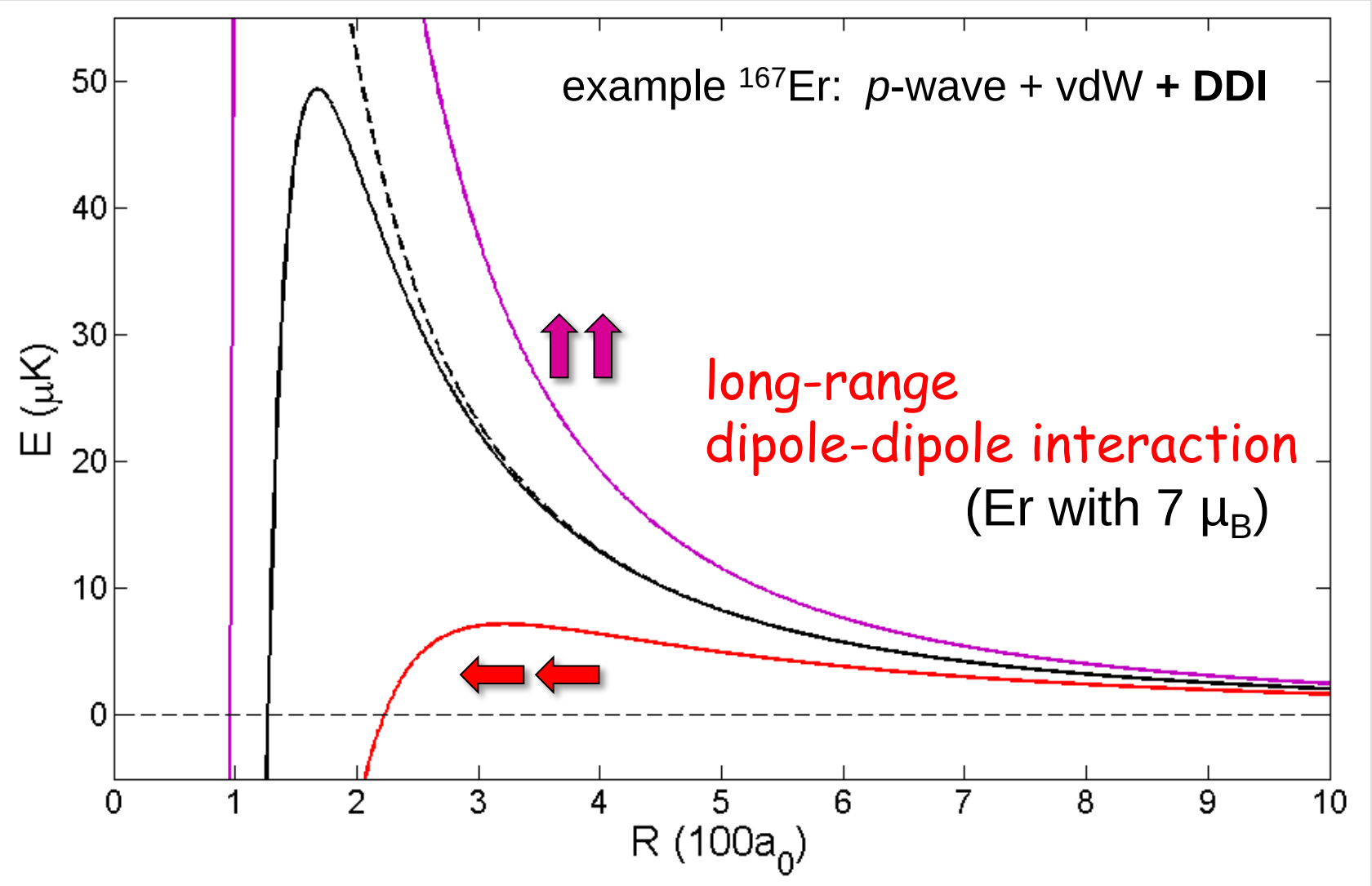

universal dipolar scattering

Bohn et al.,
NJP **11**, 055039 (2013)

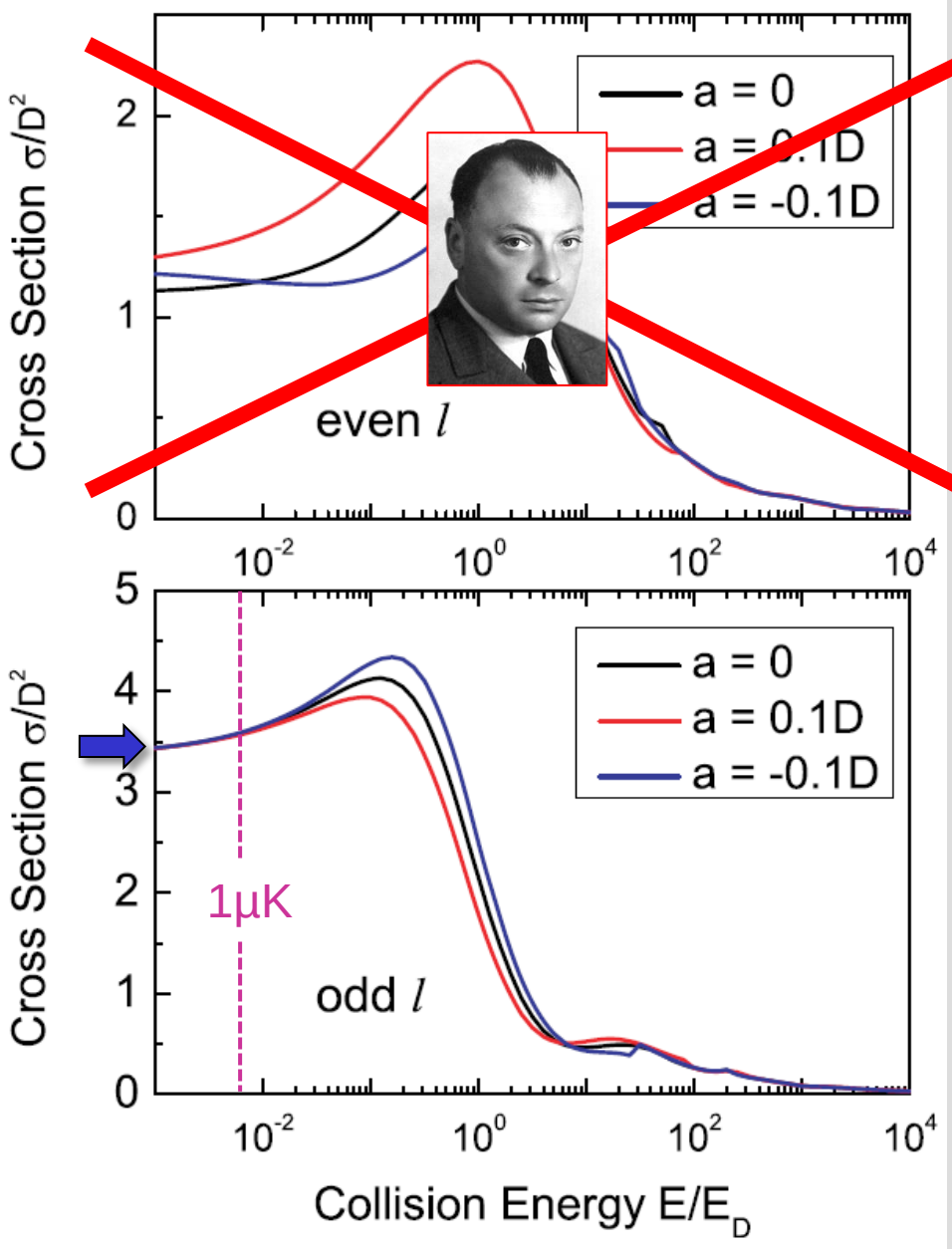

for identical fermions

threshold value
$\sigma = 6.702\, D^2$

^{167}Er

$D = 99\ a_0$
$E_D = k_B \times 210\ \mu K$

$\sigma \approx (260\ a_0)^2$

Fermi degeneracy reached ($T/T_F \approx 0.2$)

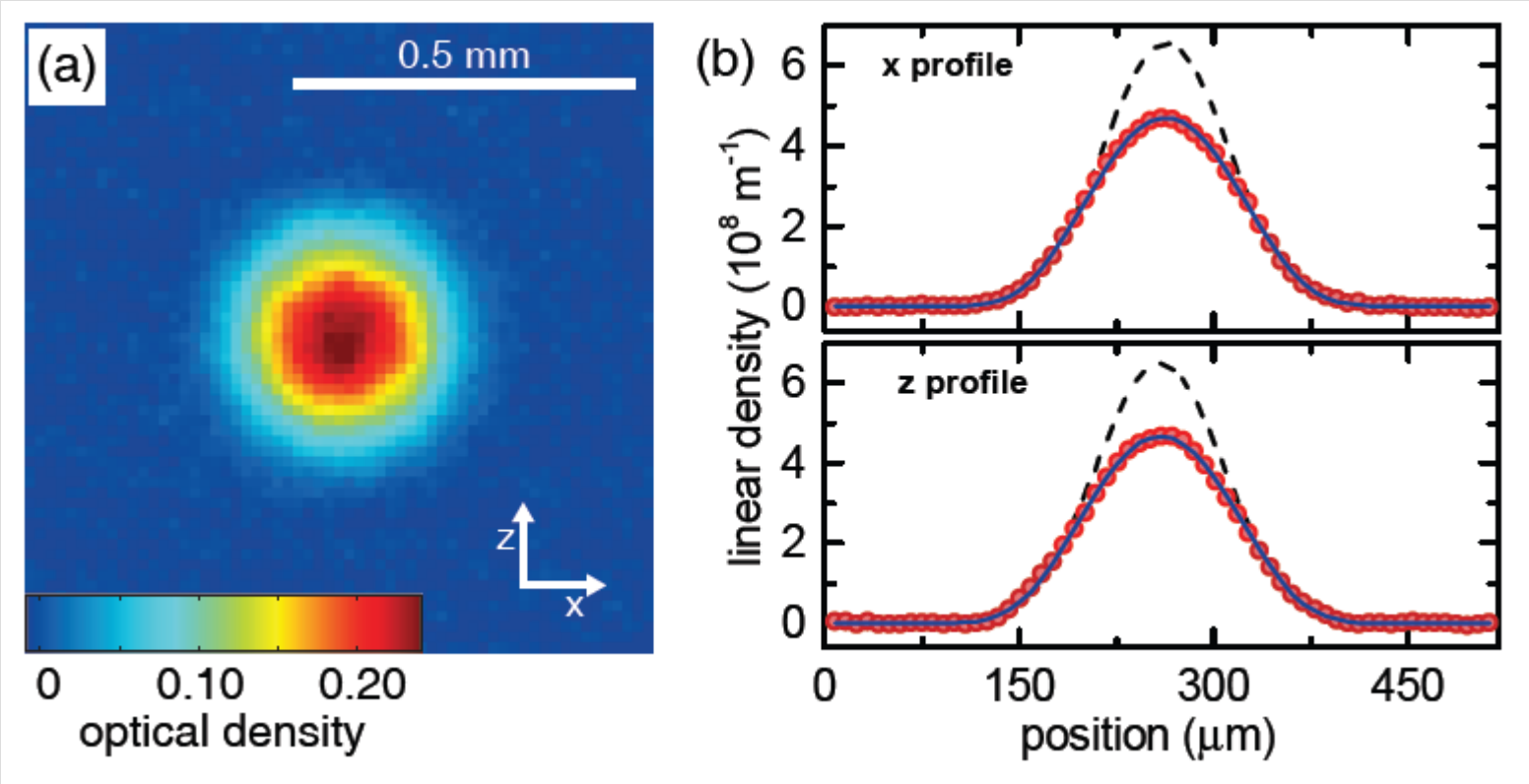

FIG. 1: (color online) Time-of-fight absorption image of a degenerate Fermi gas of Er atoms at $T/T_F = 0.21(1)$ after $t_{TOF} = 12$ ms of expansion (a) and its density distribution integrated along the z direction (upper panel) and x direction (lower panel) (b). The observed profiles (circles) are well described by fitting a poly-logarithmic function to the data (solid lines), while they substantially deviate from a fit using a Gaussian distribution to the outer wings of the cloud, i. e. w (dashed lines). The absorption image is averaged over six individual measurements.

Aikawa et al., PRL **111**, xxxxxx (2013)

highly efficient evaporative cooling

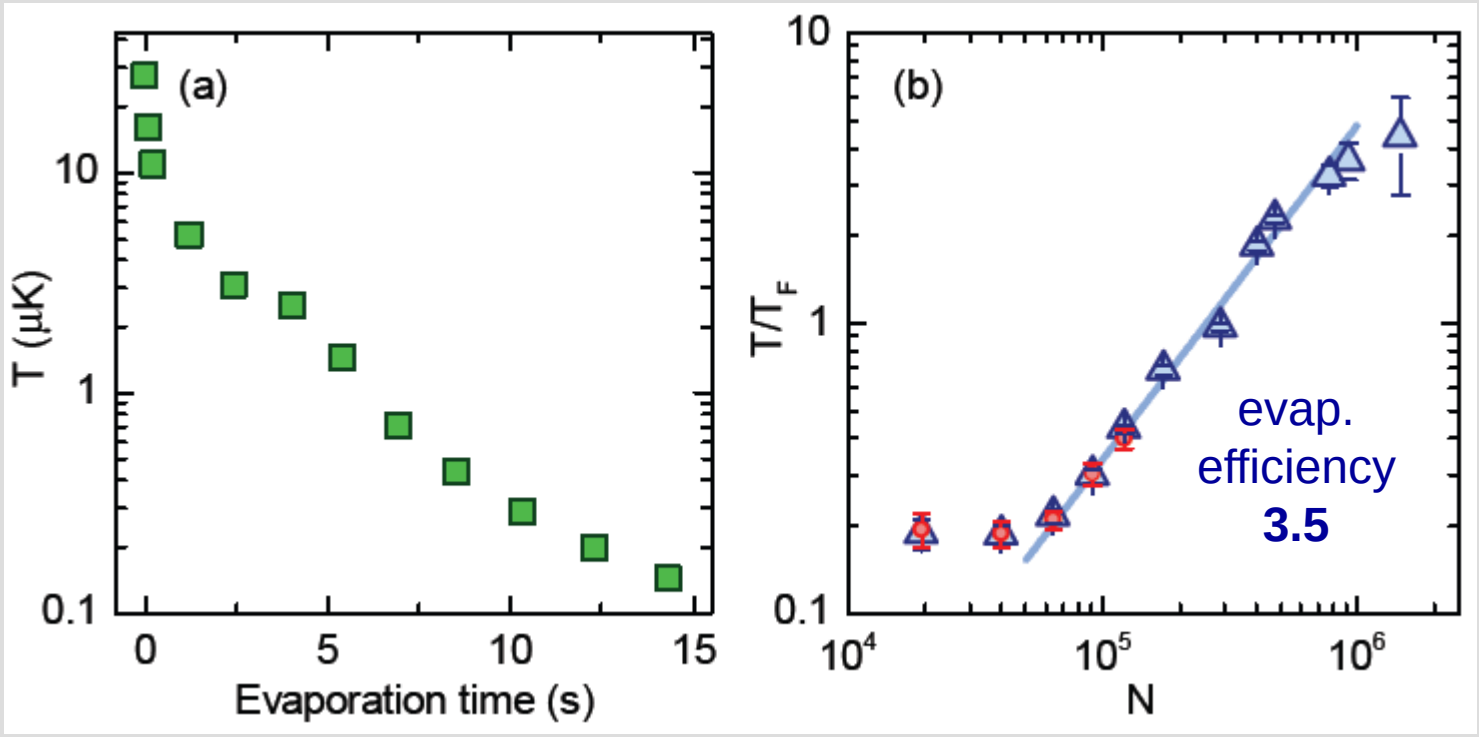

FIG. 2: (color online) Evaporation trajectory to Fermi degeneracy. (a) Temperature evolution during the evaporation ramp and (b) corresponding T/T_F versus N. The ratio T/T_F is obtained from the width σ of the distribution (triangles) and from the fugacity (circles); see text. The error bars originate from statistical uncertainties in temperature, number of atoms, and trap frequencies for the width measurements and the standard deviations obtained from several independent measurements for the fugacity. The solid line is a linear fit to the data for $0.2 < T/T_F < 4$.

Aikawa et al., PRL **111**, xxxxxx (2013)

no other spin states

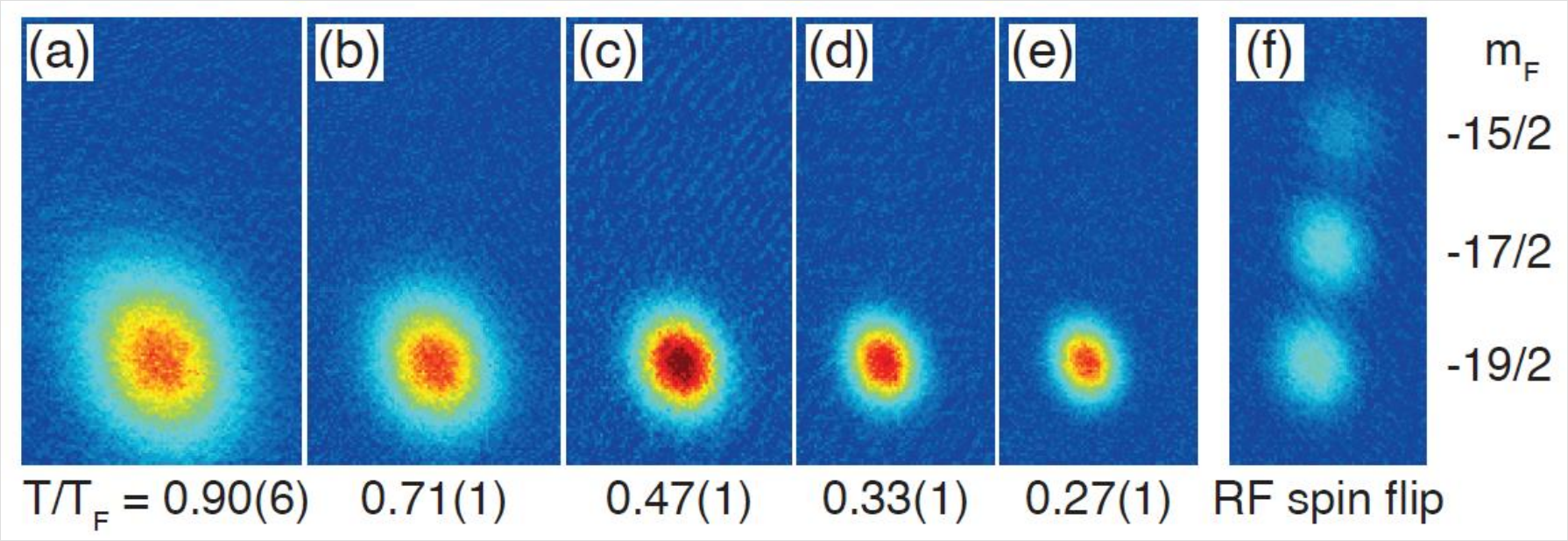

FIG. 3: (color online) Absorption images of the atomic cloud with a Stern-Gerlach separation of the spin components. A magnetic field gradient of about 40 G/cm is applied during the expansion for about 7 ms. (a)-(e) Along the entire evaporative cooling sequence, atoms are always spin-polarized in the lowest hyperfine sublevel $|F = 19/2, m_F = -19/2\rangle$. T/T_F of the atomic samples are indicated in each panel. In (f) the image is obtained right after RF mixing of the spin states for the sample at $T/T_F = 0.33(1)$. The three clouds correspond to the magnetic sublevels $m_F = -19/2, -17/2$, and $-15/2$ from bottom to top.

Aikawa et al., PRL **111**, xxxxxx (2013)

cross section confirmed

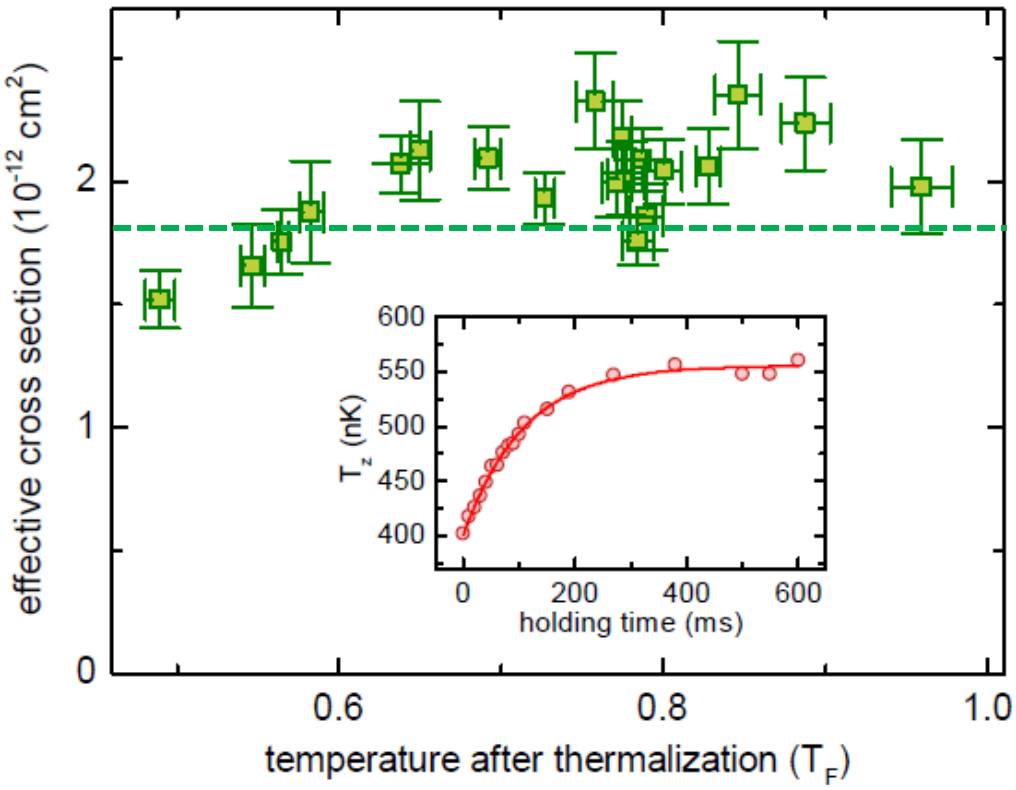

FIG. 4: (color online) Effective elastic cross-section as a function of T/T_F after thermalization. In the non-degenerate regime, the effective cross section is constant and gives a mean value of $2.0(5) \times 10^{-12}\text{cm}^2$. The error bars for each point contain the statistical uncertainties of the time constant for cross-dimensional thermalization, of the trap frequencies, and of the temperature. A typical cross-dimensional thermalization measurement with an exponential fit to the data is shown in the inset. T_z is the temperature along the z-direction.

Aikawa et al., PRL **111**, xxxxxx (2013)

some interesting numbers

optical dipole trap (1570nm light): $\bar{\omega}/2\pi = 380$ Hz *tight!*

number of atoms
$N \approx 6 \times 10^4$

Fermi temperature
$T_F = k_B \times 1.3\ \mu K$

peak number density
$\boldsymbol{n = 4 \times 10^{14}\ cm^{-3}}$

three-body decay rate
$\boldsymbol{L_3 < 3 \times 10^{-30}\ cm^6/s}$

facilitates highly efficient evaporative cooling

physics behind that?

centrifugal barrier: two regimes

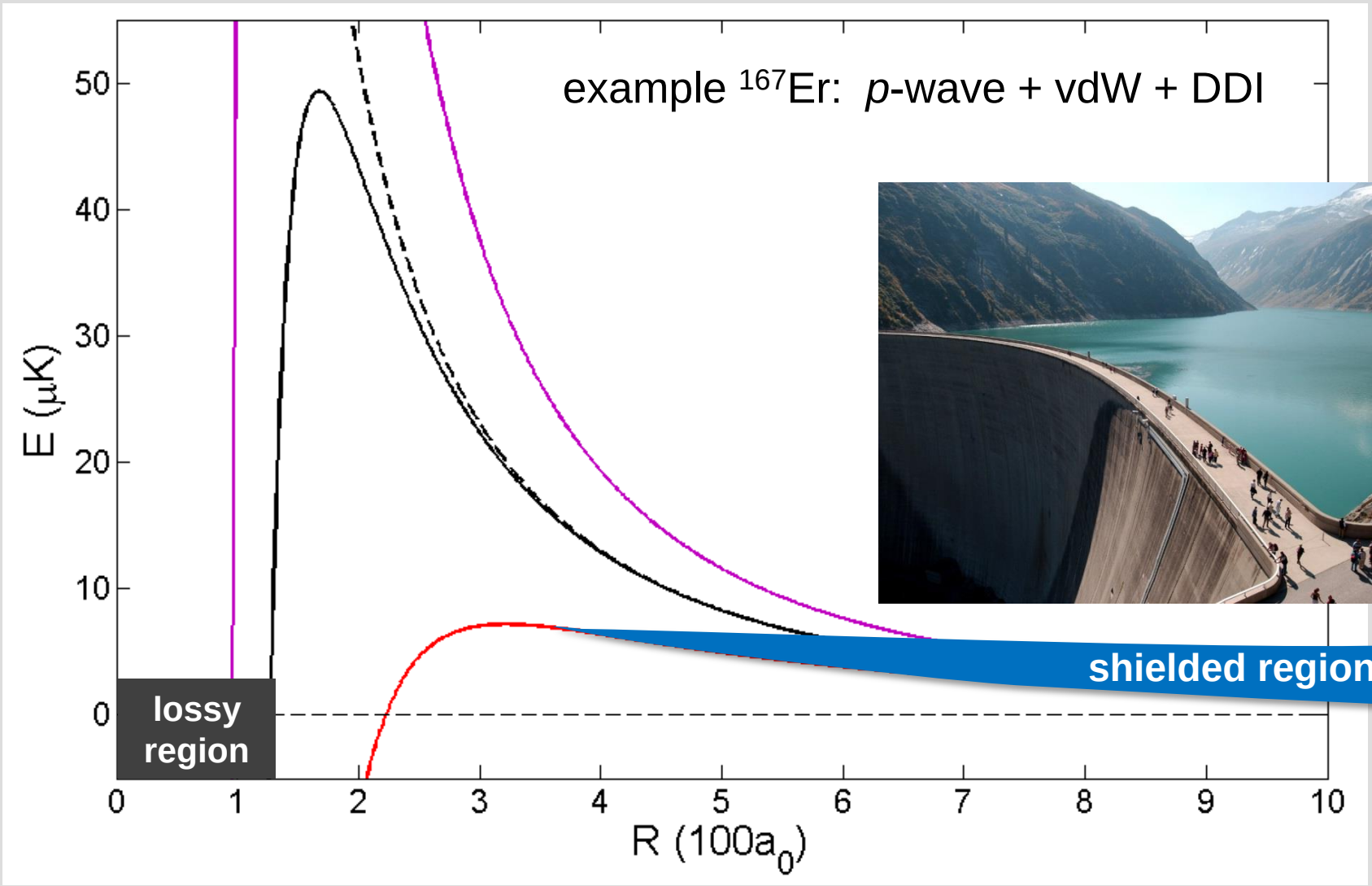

optimum DDI strength

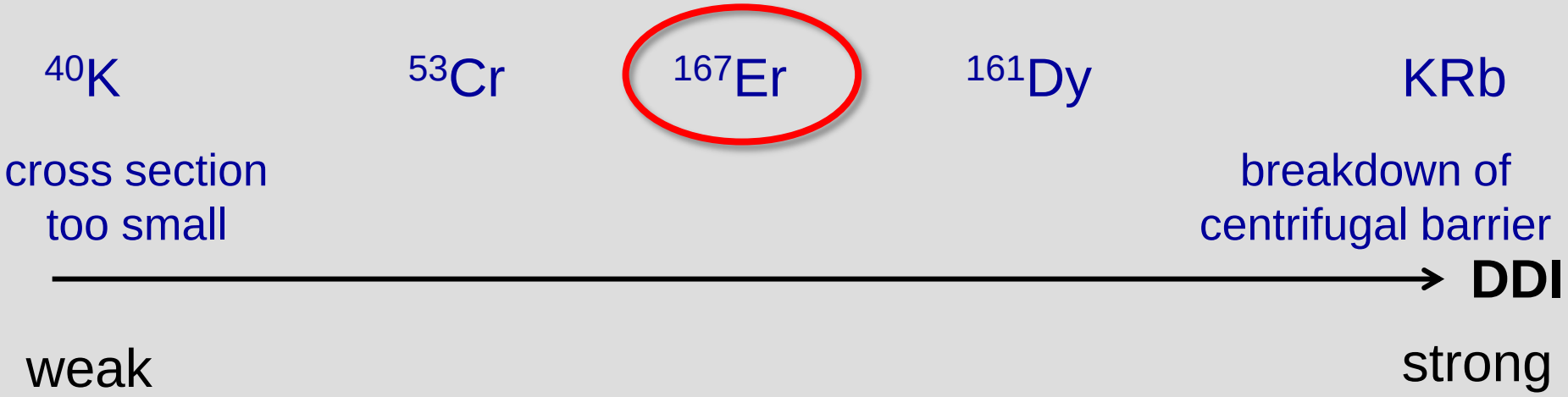

outlook

extreme number densities:

- what is the limit?
- p-wave superfludity??

- trimer or N-body states?

other systems:

- stable fermionic Feshbach molecules

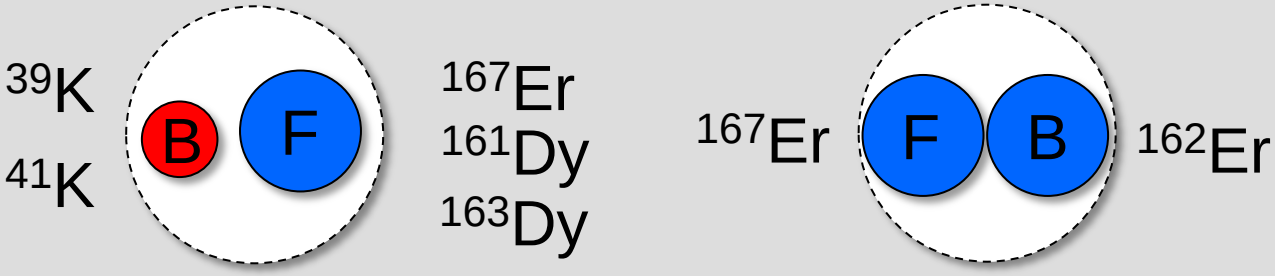

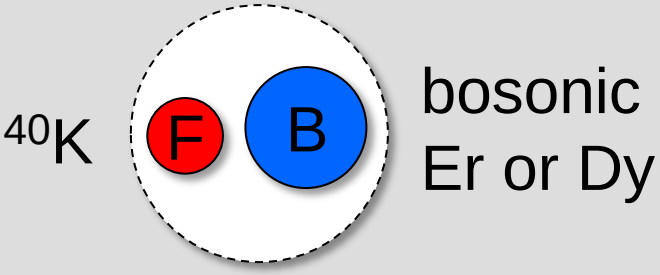

three-body physics of two-fermion systems

J. Phys. B: At. Mol. Opt. Phys. 40, 1429 (2007)

Kartavtsev-Malykh trimer

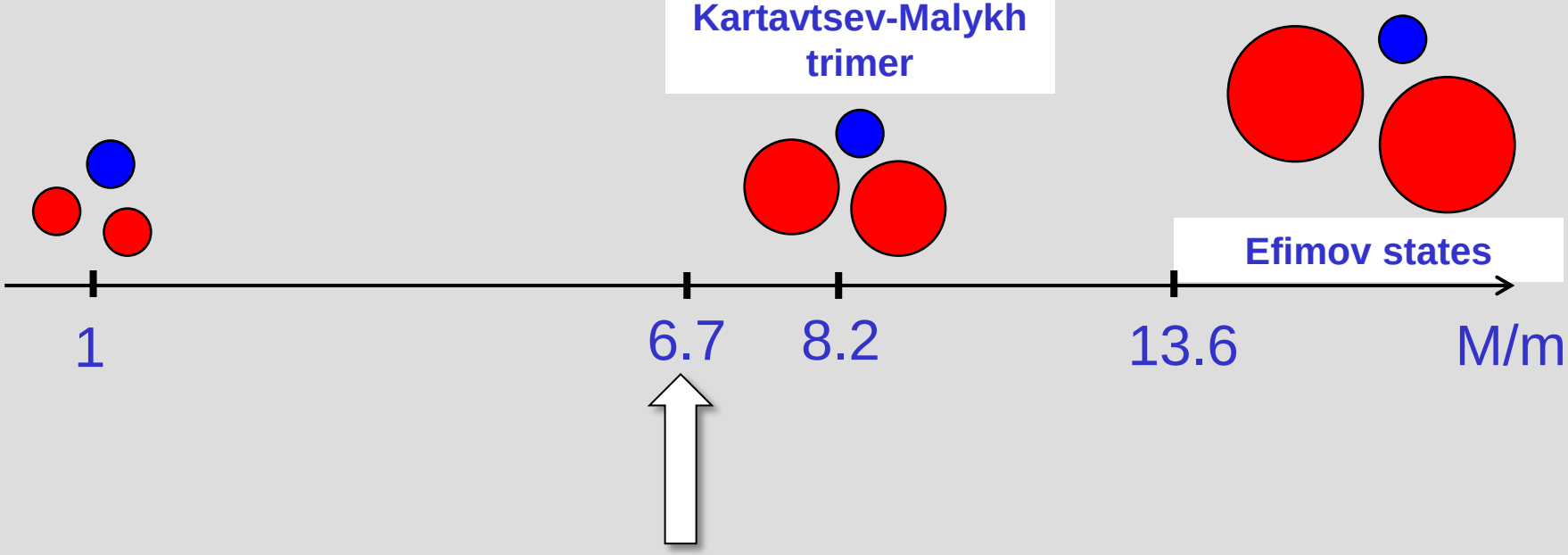

we are here !
^{40}K - ^{6}Li

atom-dimer scattering

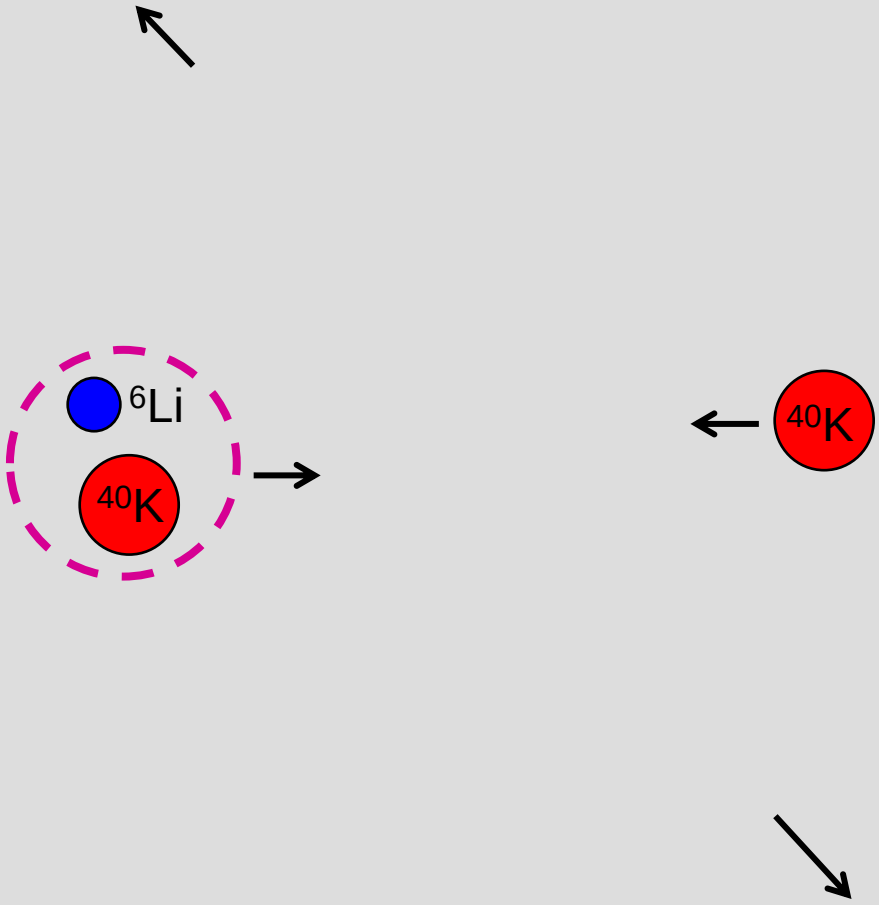

three-body process

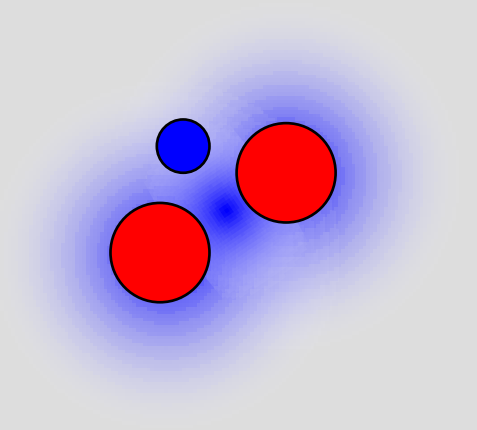

Levinsen, Tiecke, Walraven, Petrov, PRL **103**, 153202 (2009)

Levinsen, Petrov, EPJD **65**, 67 (2011)

see also Alzetta, Combescot, Leyronas, PRA **86**, 062708 (2012)

Born-Oppenheimer 3-body potentials

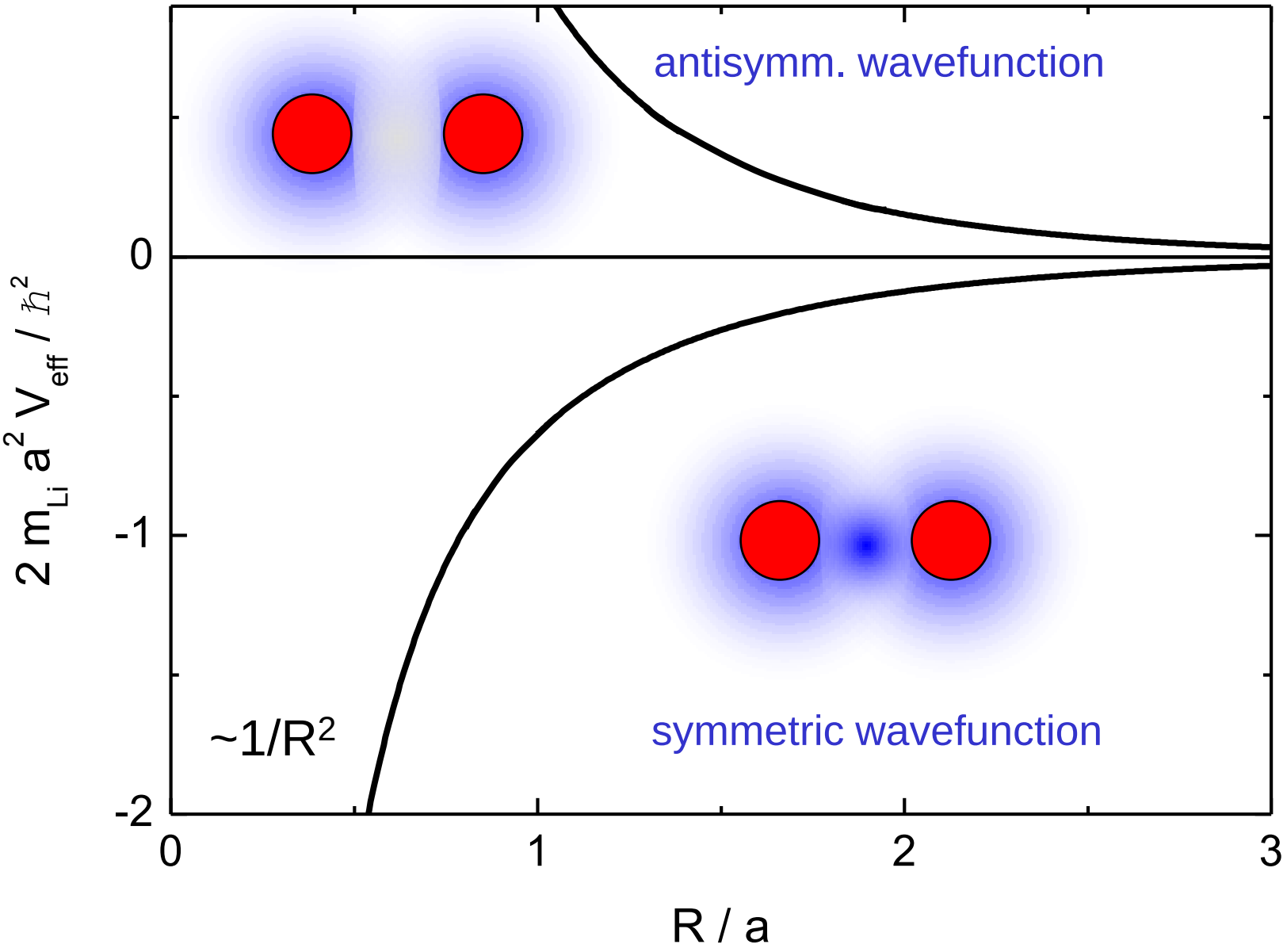

symmetry of AD wavefunction

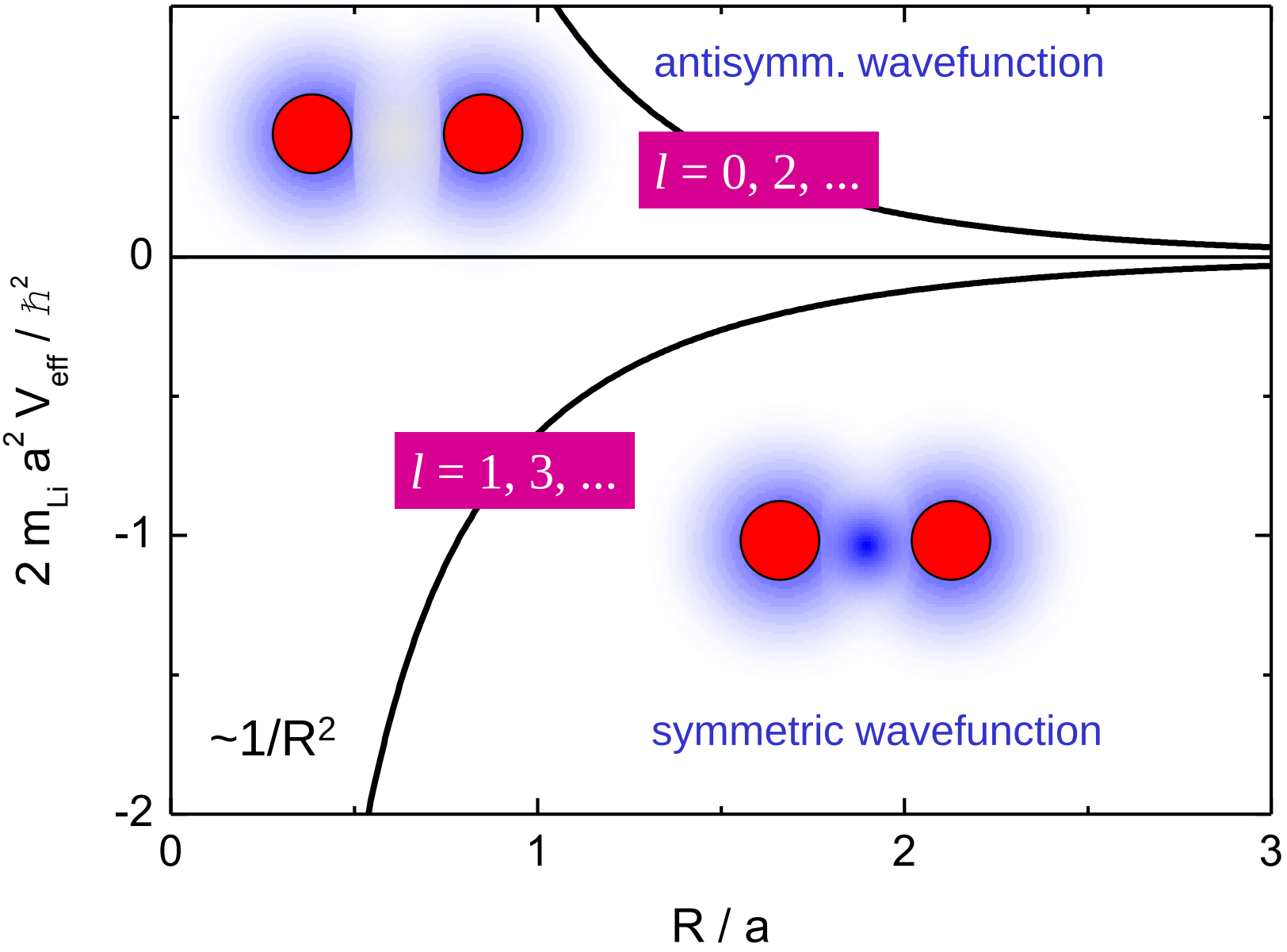

effective potentials in partial-wave channels

for 155G Li-K Feshbach resonance (880mG wide)

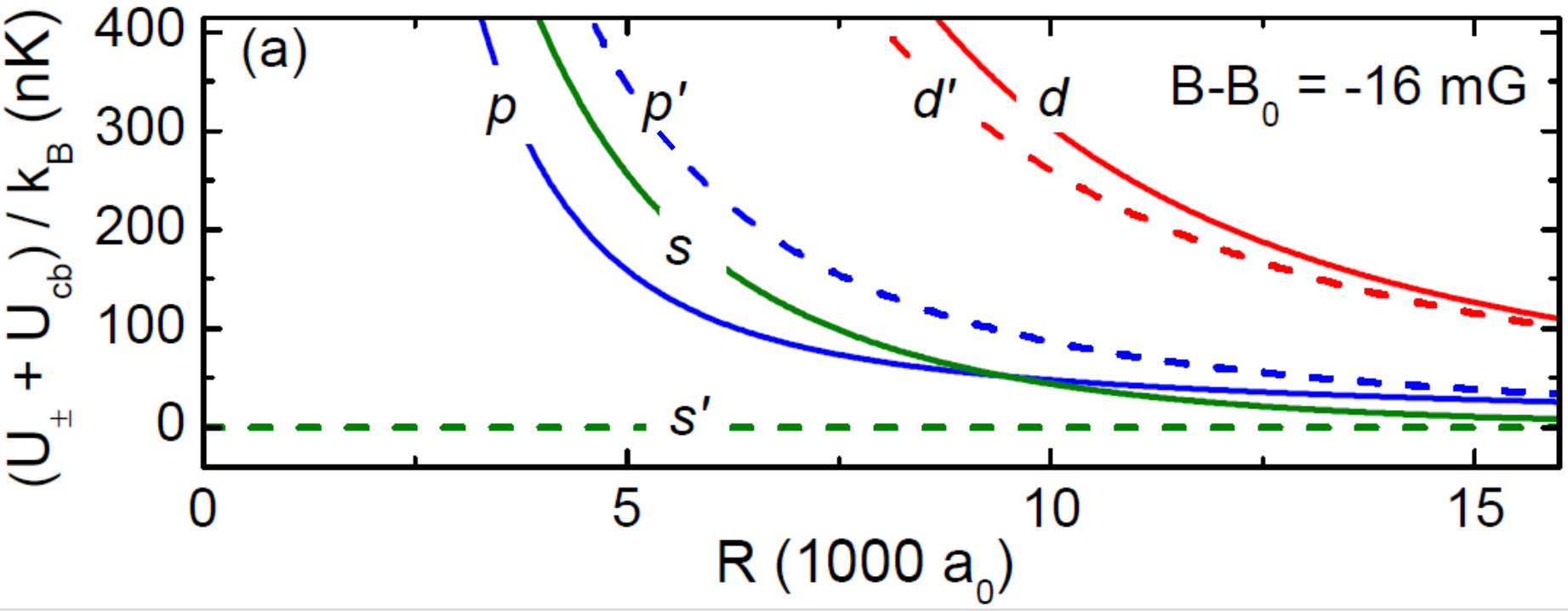

strong effect on *p*-wave barrier

strong atom-dimer attraction!

scattering amplitude

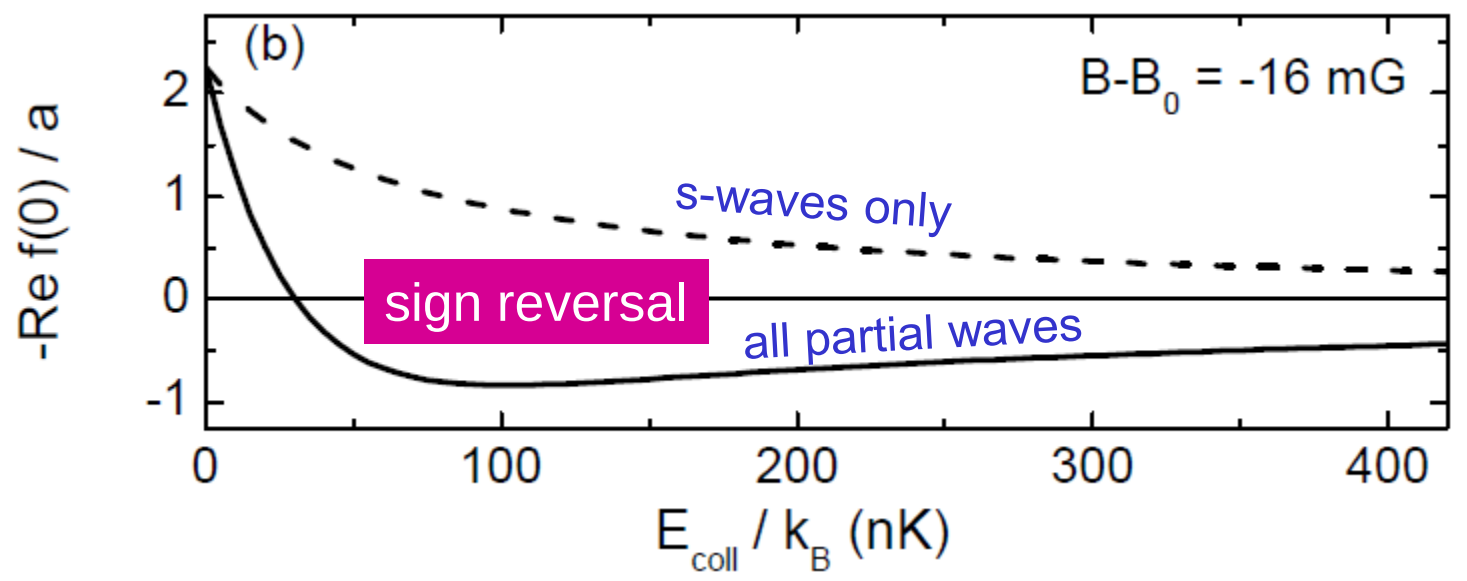

scattering amplitude

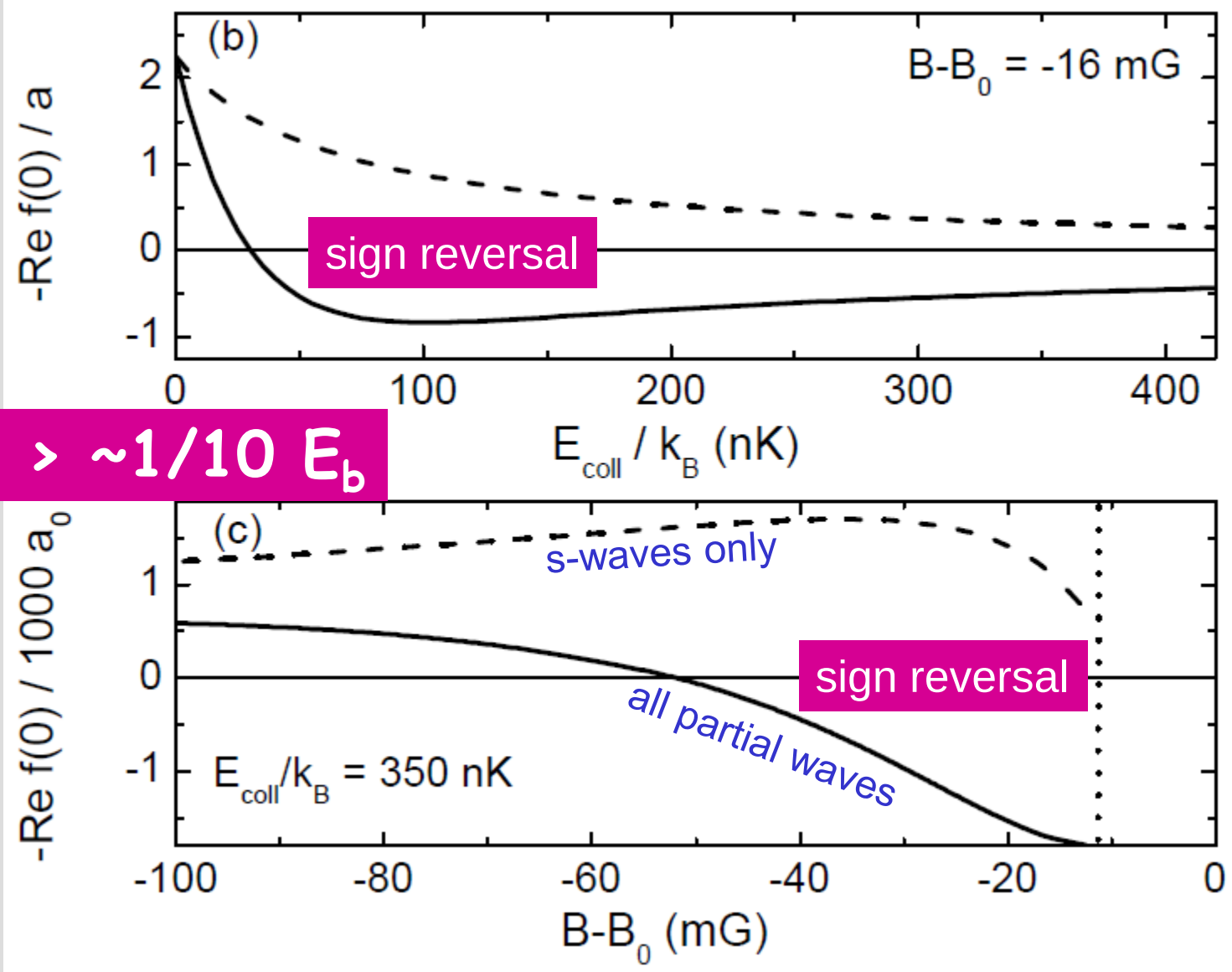

E_{coll} > ~1/10 E_b

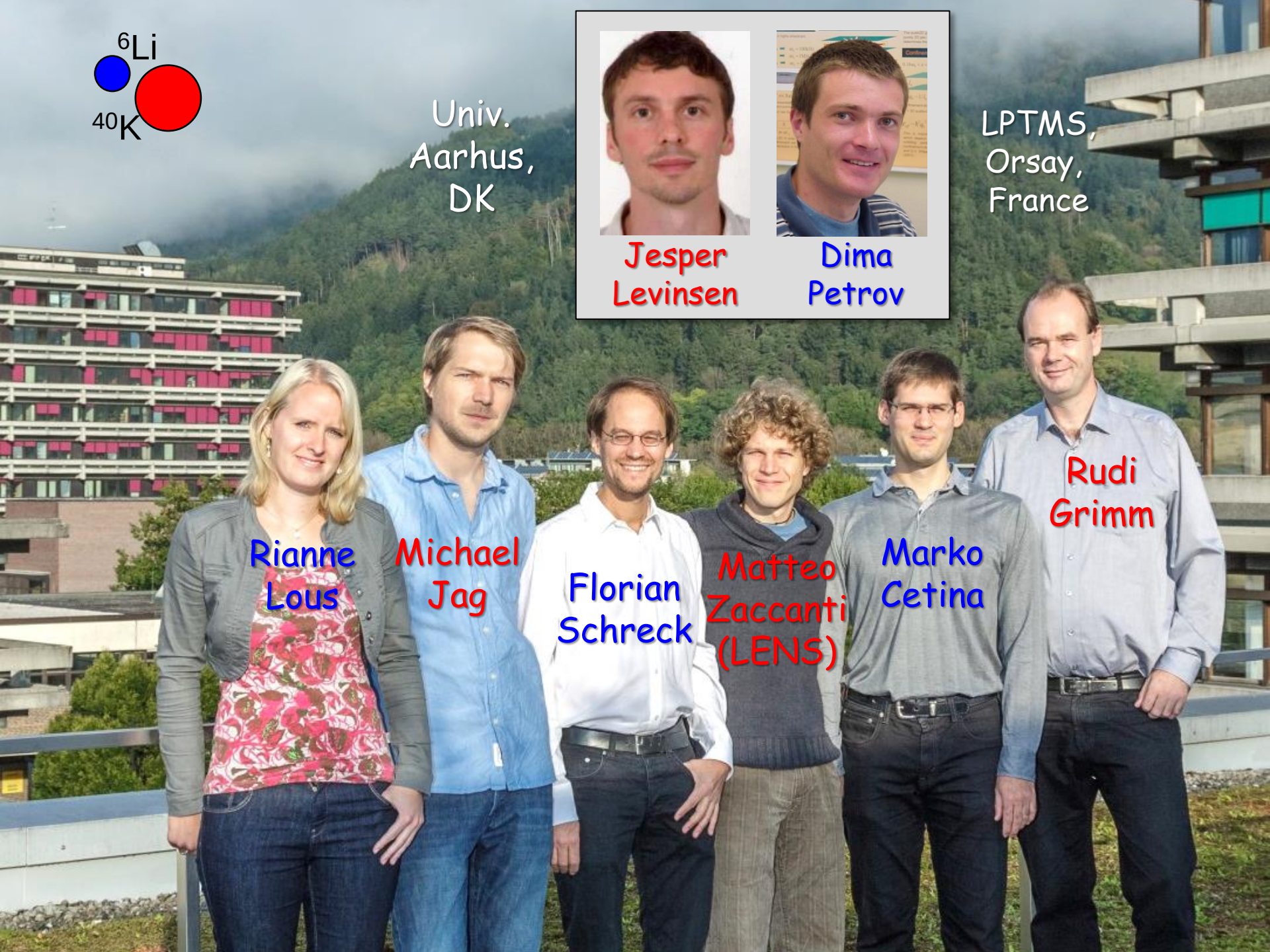
^{6}Li
^{40}K
Univ. Aarhus, DK
LPTMS, Orsay, France
Jesper Levinsen
Dima Petrov
Rianne Lous
Michael Jag
Florian Schreck
Matteo Zaccanti (LENS)
Marko Cetina
Rudi Grimm

mixture of heavy and light fermions: ^{40}K-^{6}Li

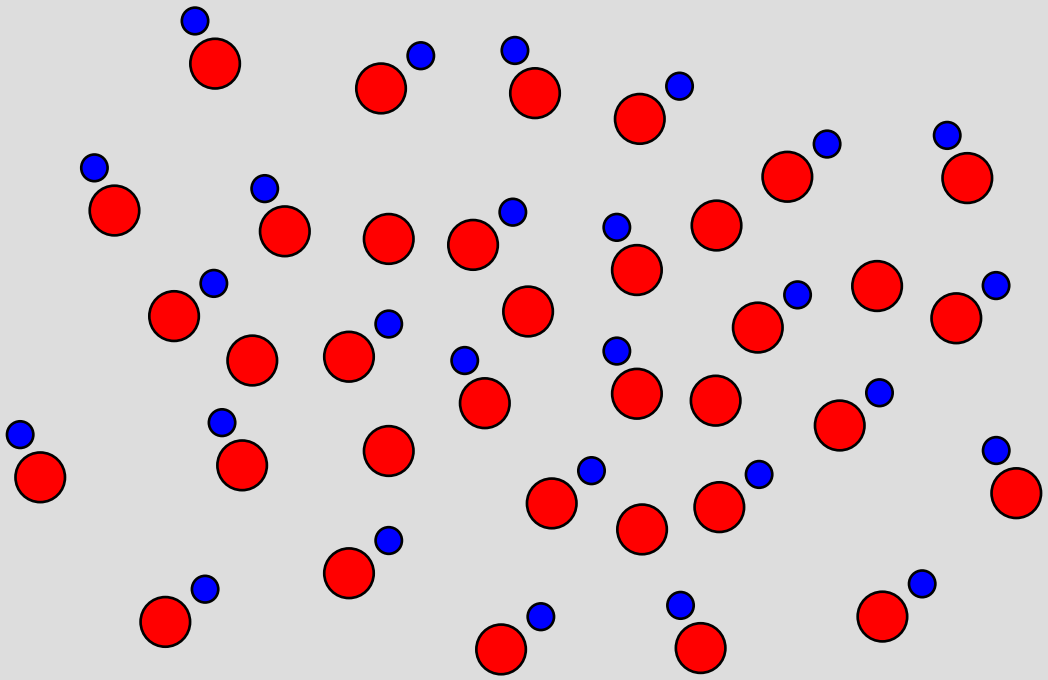

making weakly bound dimers (a>0)

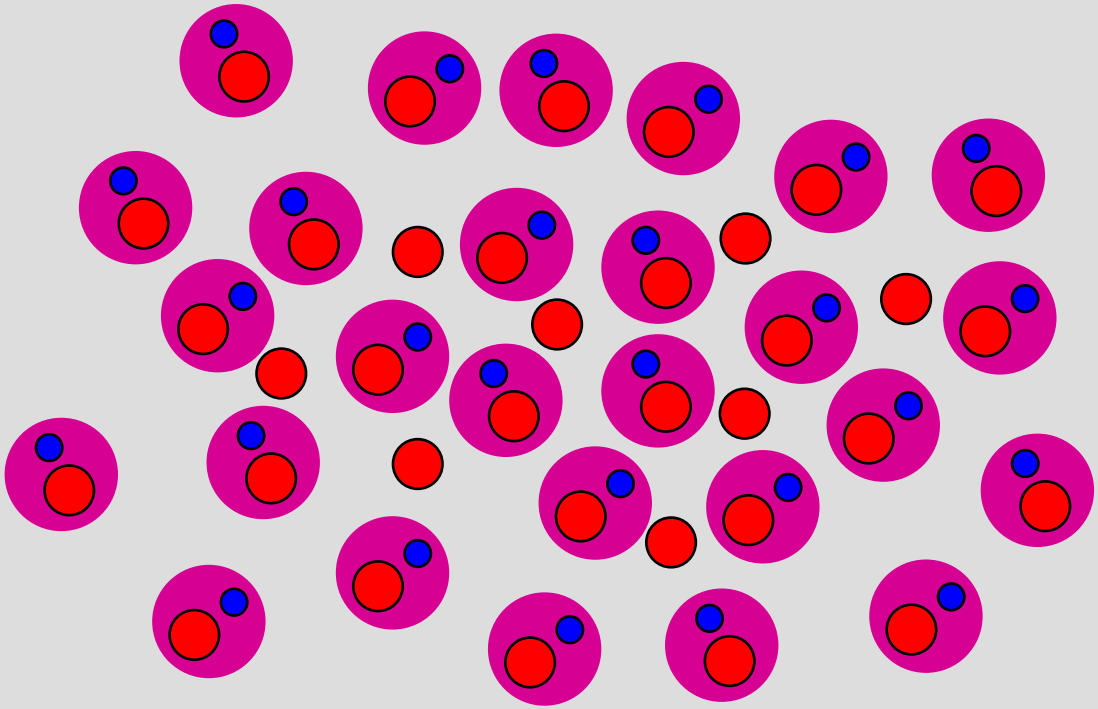

flipping the spin state of the free atoms

^{40}K interacting spin state

non-interacting spin state

rf coupling

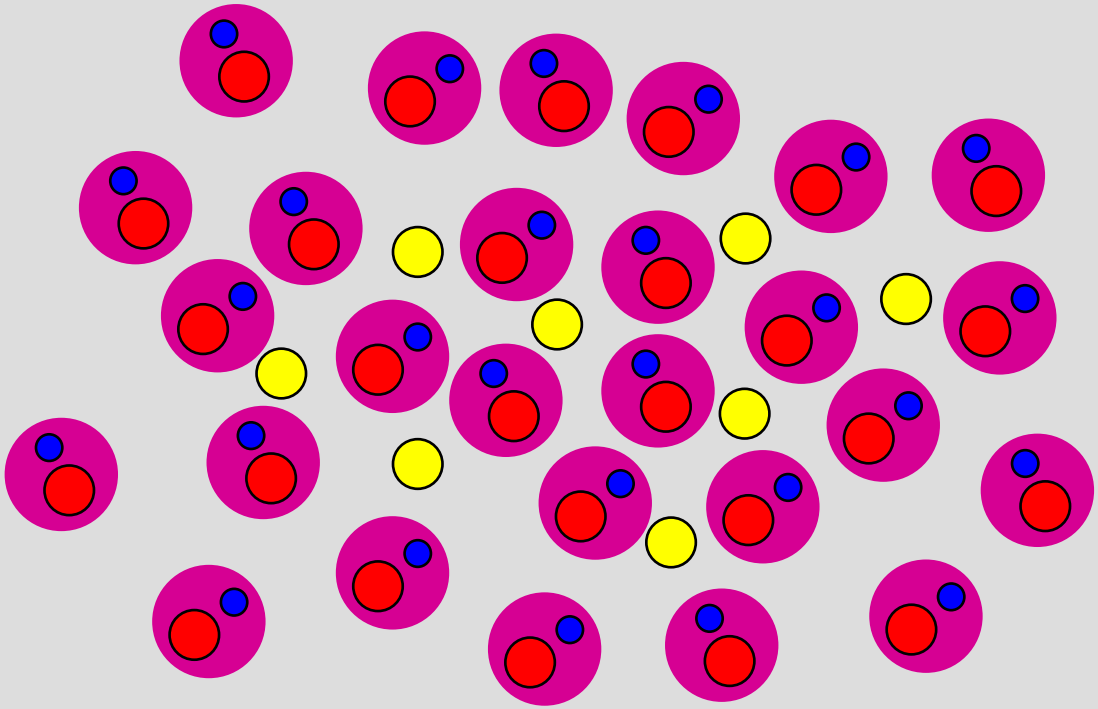

flipping the spin state of the free atoms

^{40}K interacting spin state

non-interacting spin state

rf coupling

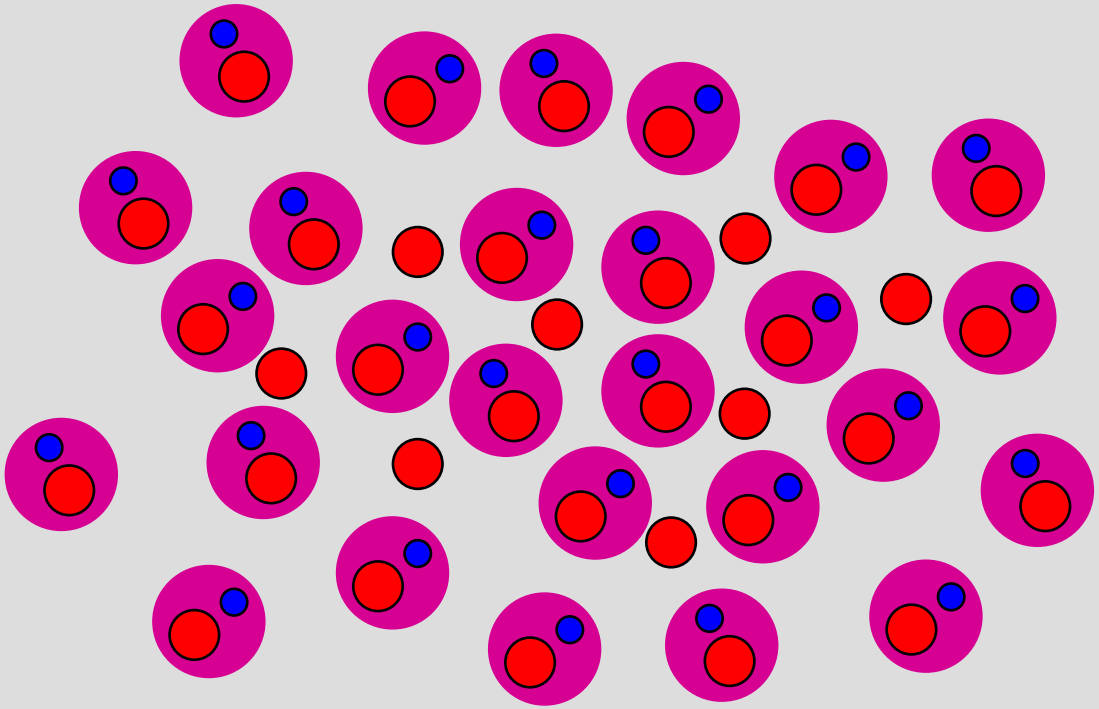

flipping the spin state of the free atoms

^{40}K interacting spin state

non-interacting spin state

rf coupling

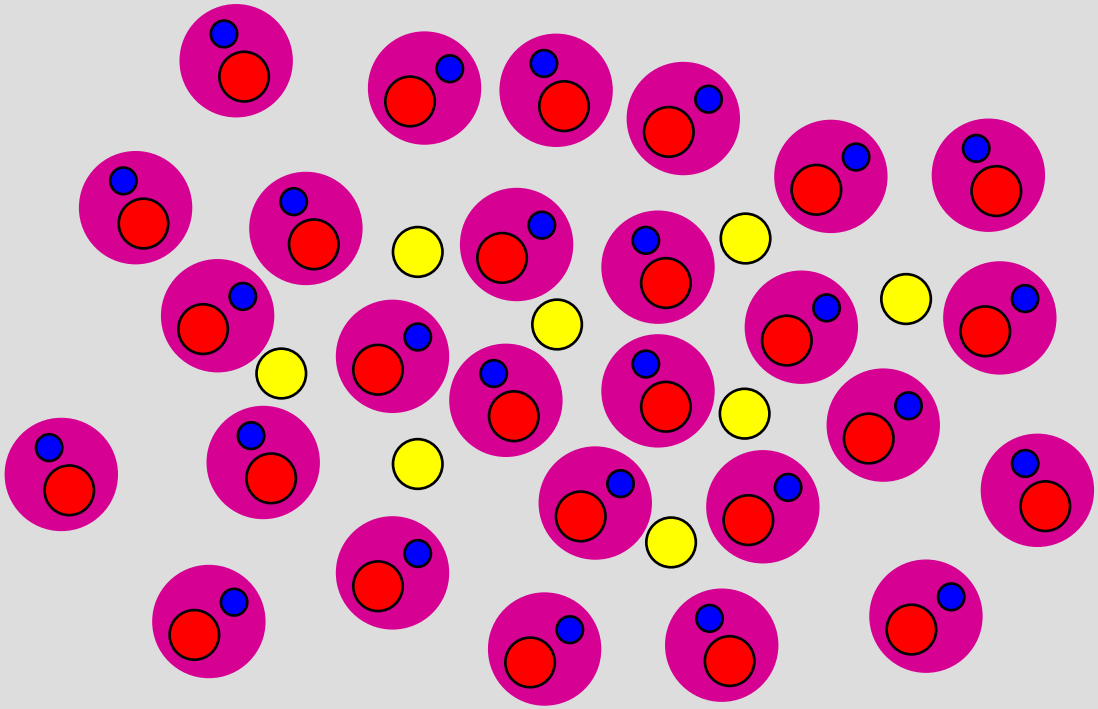

radio-frequency spectroscopy

interacting spin state

non-interacting spin state

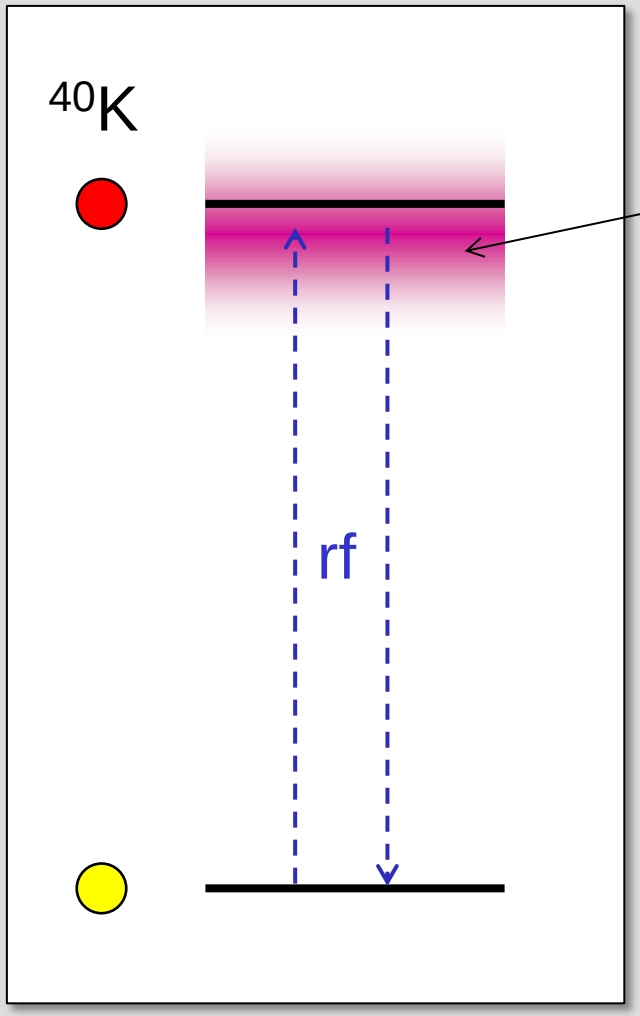

interaction with ^{6}Li^{40}K dimers

excellent tool to probe interaction shifts !!!

sample rf spectra

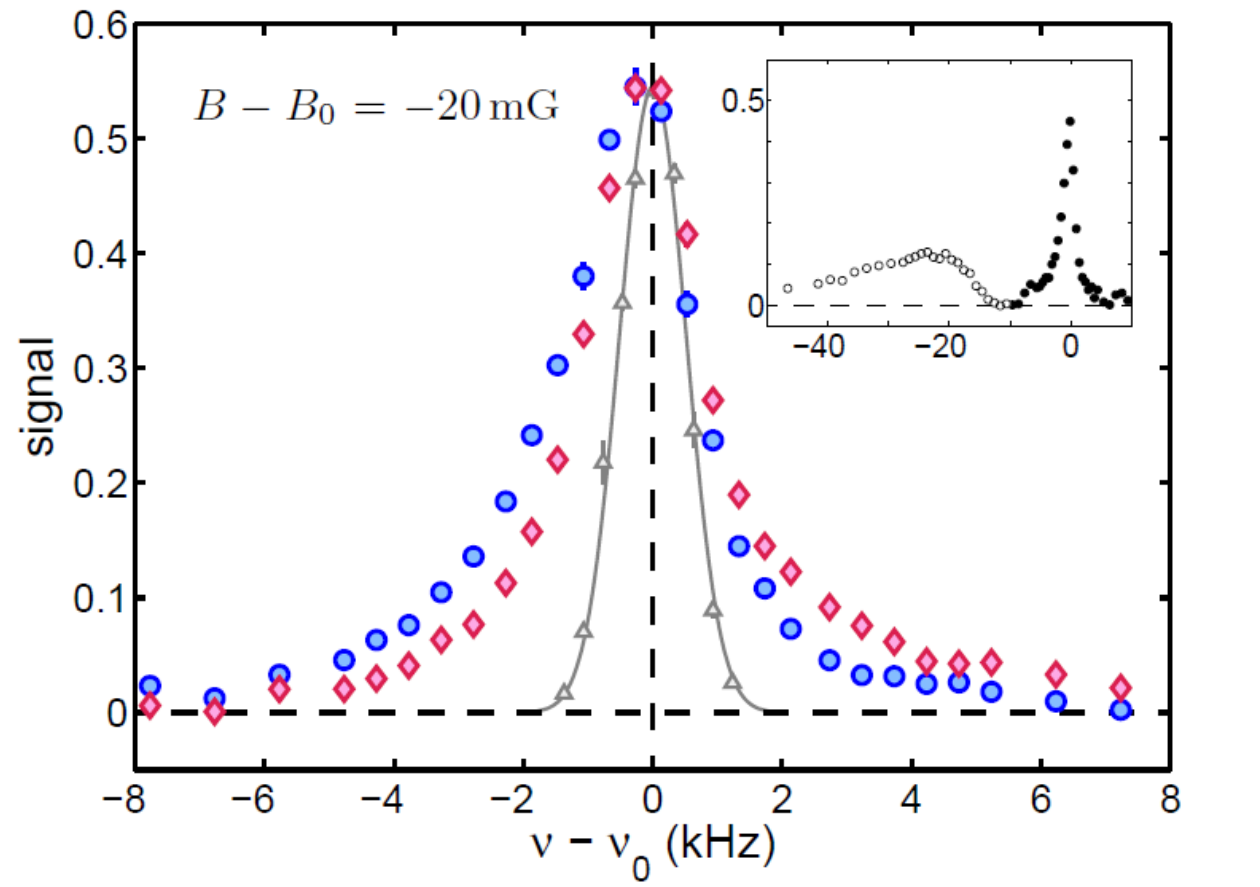

broadening and shift

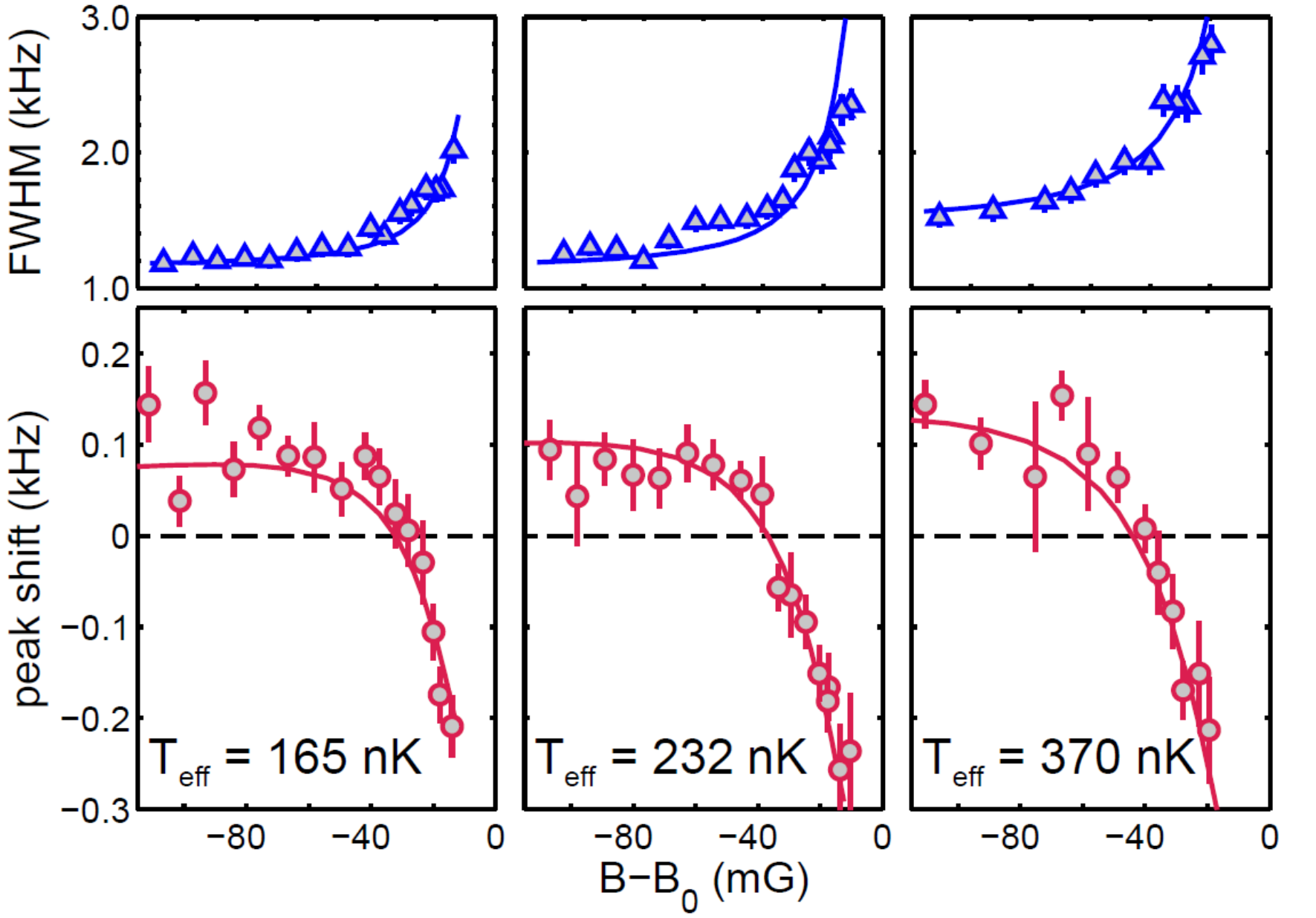

sign reversal

$\delta\nu = \hbar\bar{n}_{\mathrm{D}} a_{\mathrm{eff}} / \mu_3$ shift in terms of eff. sc. length

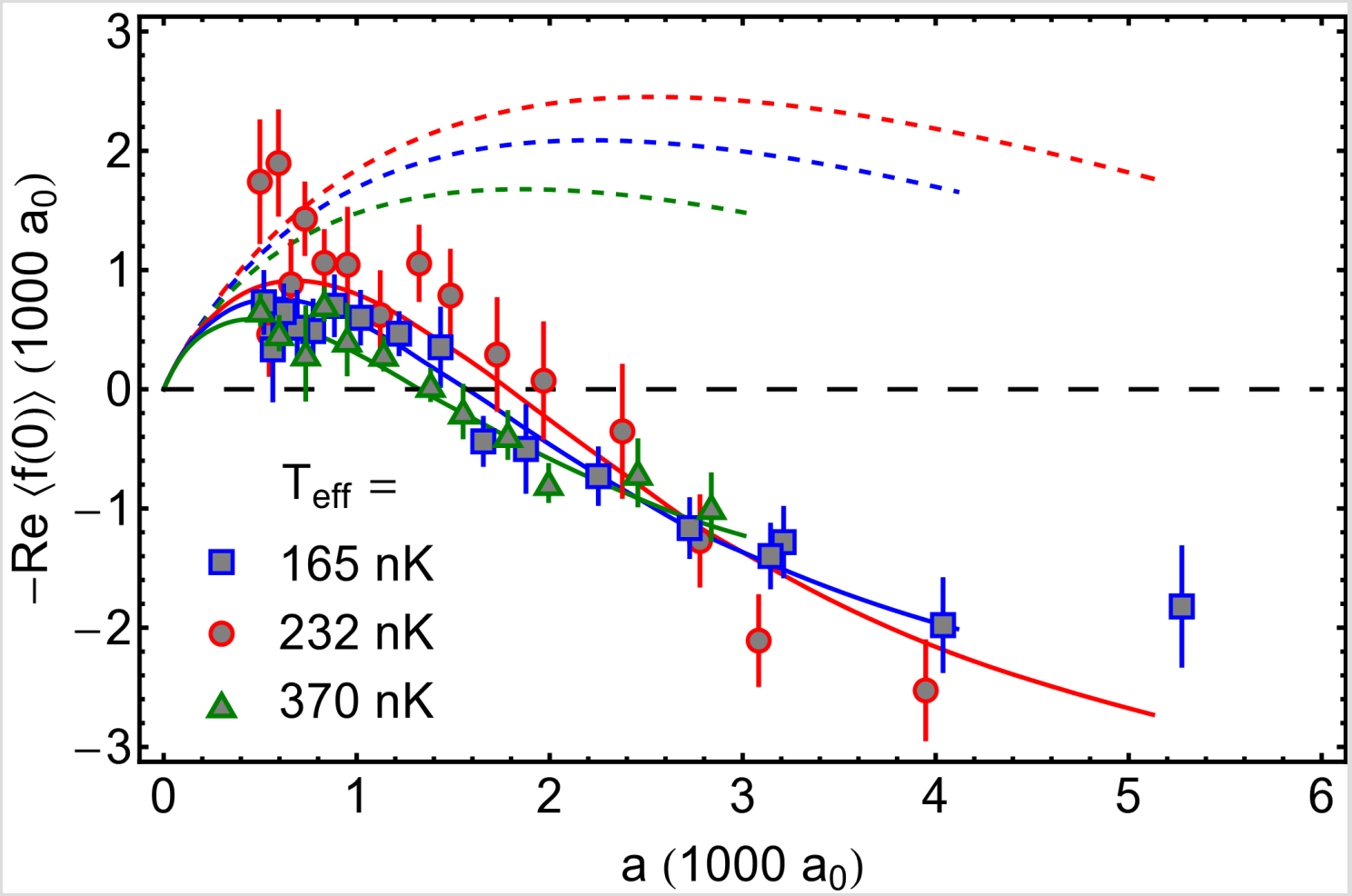

why we are so excited!

mass imbalance: **qualitatively new** interaction properties

no-loss few-body effect

ultracold **paradigm shift**: physics beyond s-waves

potentially strong impact on many-body physics !!!

strongly interacting, mass-imbalanced mixtures

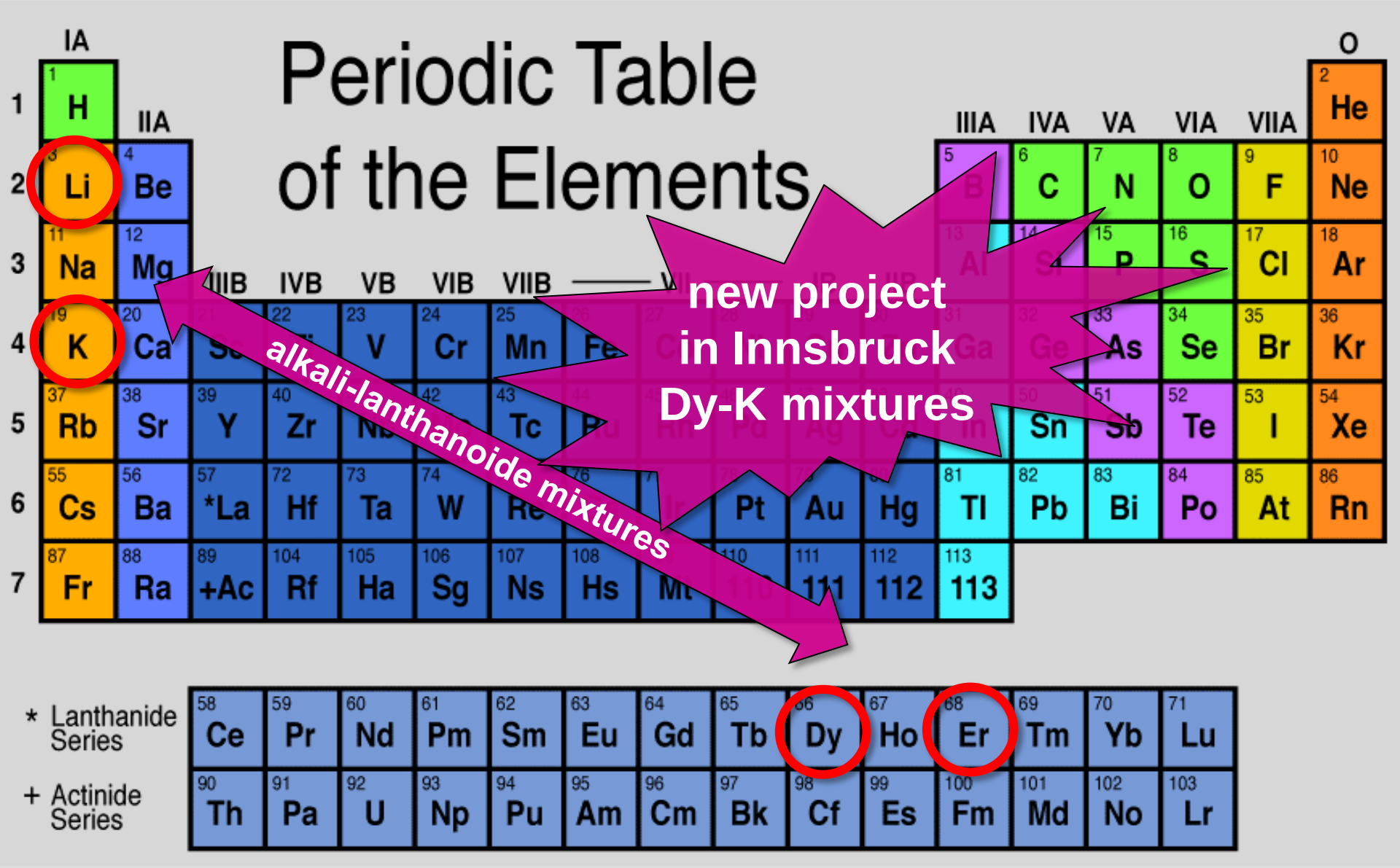


universität
innsbruck
IQI
thank you for your
attention
FWF
Der Wissenschaftsfonds.
SFB
FoQuS
Foundations and
Applications of
Quantum Science